CALETによる
マルチメッセンジャー観測

CALET

Calorimetric Electron Telescope

鳥居祥二
Shoji Torii
Waseda University, Japan
for the CALET Collaboration

CALET Payload

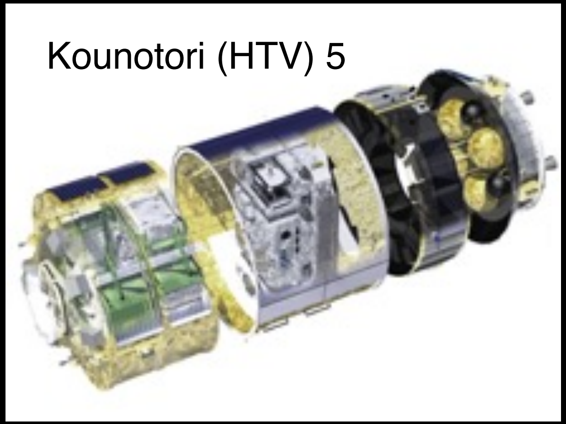

Launched on Aug. 19th, 2015 by the Japanese H2-B rocket

Emplaced on JEM-EF port #9 on Aug. 25th, 2015

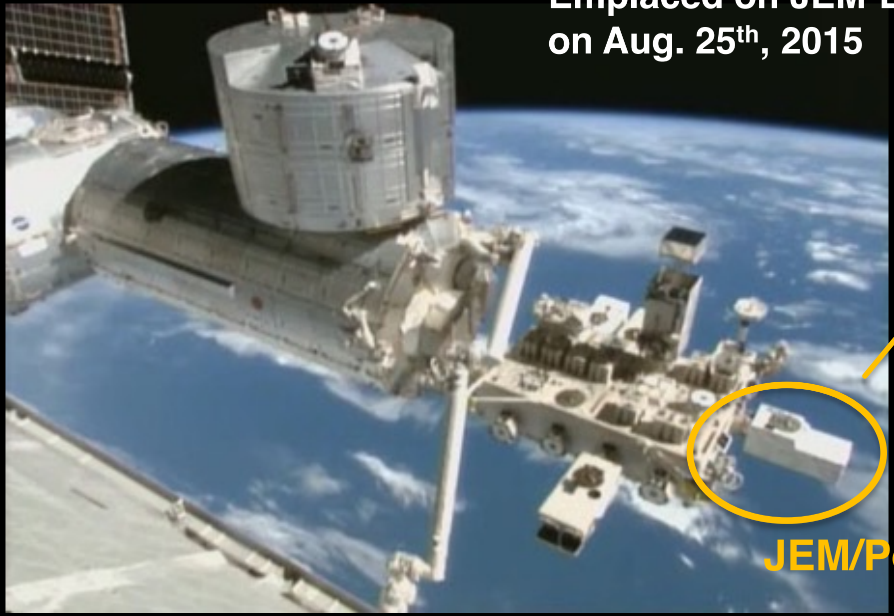

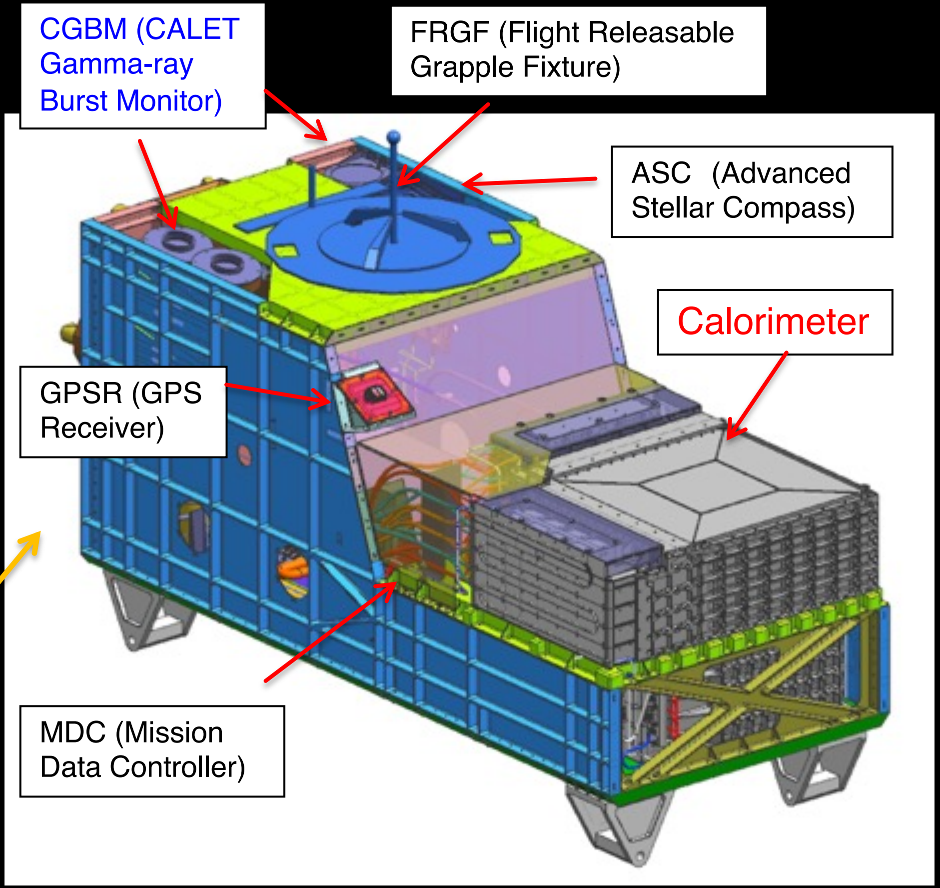

- **Mass: 612.8 kg**
- **JEM Standard Payload Size:**
  1850mm(L) × 800mm(W) × 1000mm(H)
- **Power Consumption: 507 W（max）**
- **Telemetry:**
  Medium 600 kbps (6.5GB/day) / Low 50 kbps

Cosmic Ray Observation with CALET on the ISS

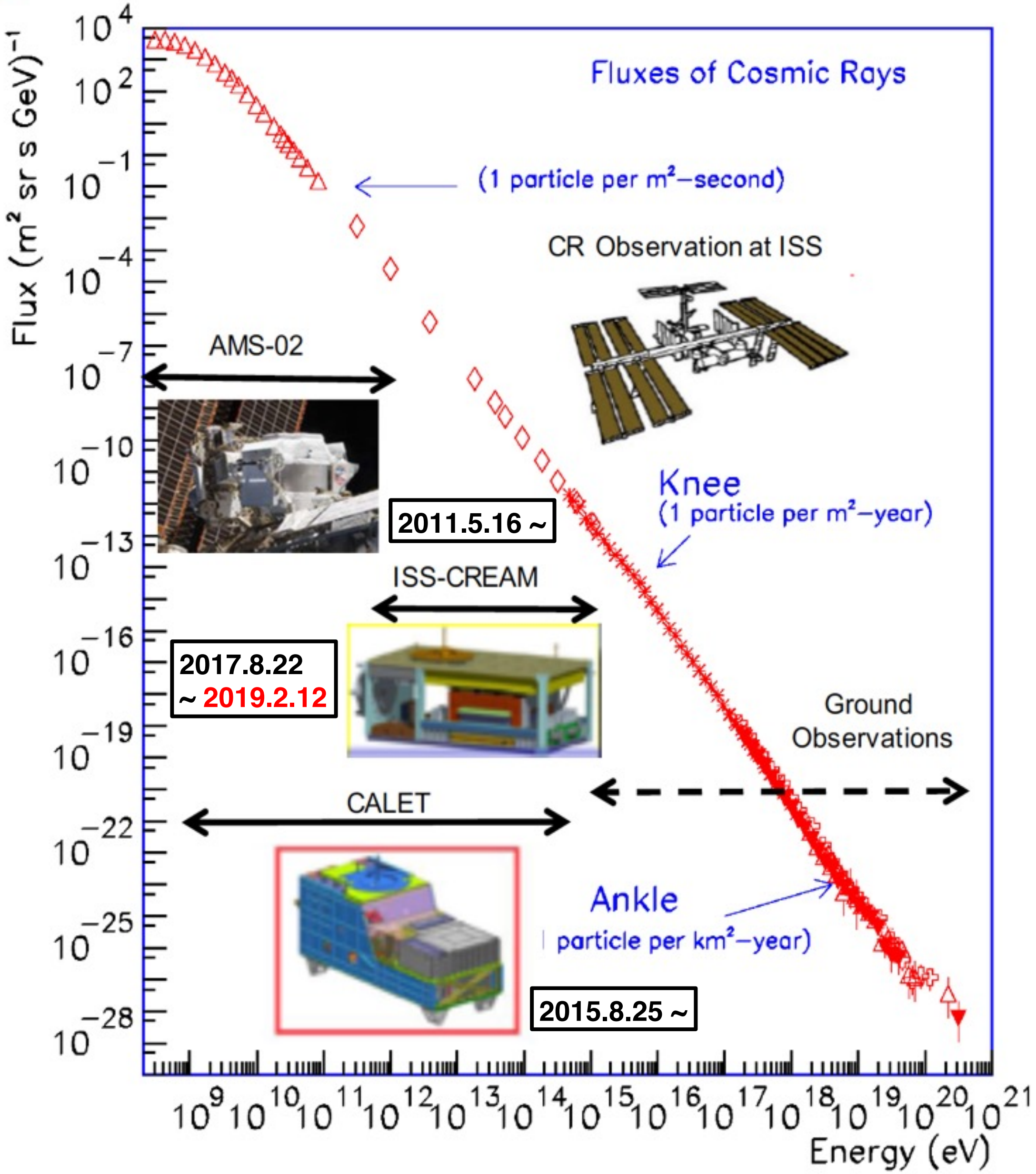

Overview of CALET Observations

- Direct cosmic ray observations in space at highest energy region.
- Cosmic ray observation at world-record level using a large-scale detector at the ISS over a long-term more than 8 years.
- Electron observation in 1 GeV - 20 TeV is achieved with high energy resolution due to optimization for electron detection
  ⇨ Search for Dark Matter and Nearby Sources
- Observation of cosmic-ray nuclei will be performed in energy region from 10 GeV to 1 PeV
  ⇨ Unravelling the CR acceleration and propagation mechanism
- Detection of transient phenomena in space by stable observations
  ⇨ Gamma-ray burst, Solar flare, EM radiation from GW sources etc.

Cosmic Rays and Multi-Messanger Observations

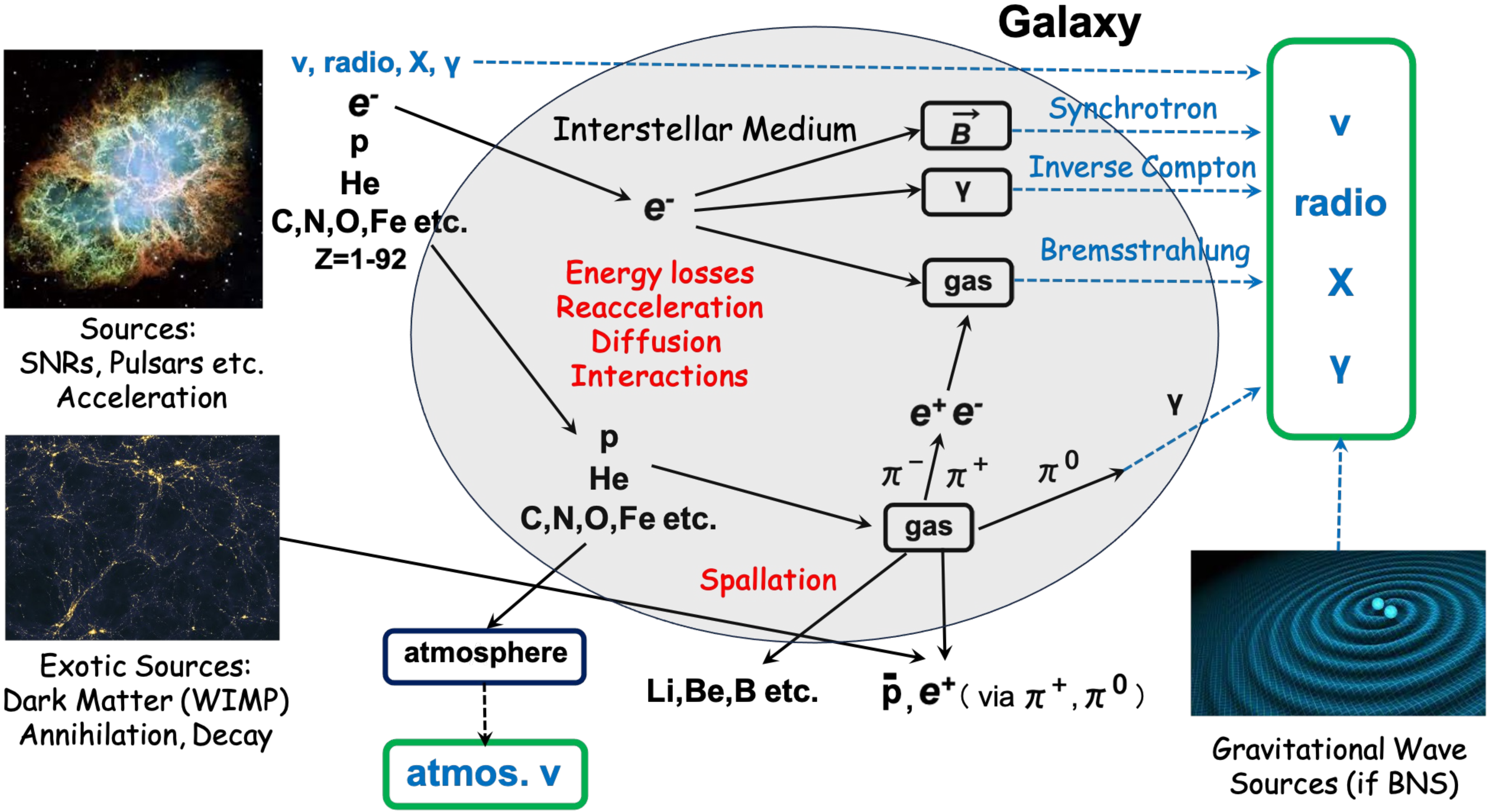

Overview of the CALET Calorimeter

Field of view: ~ 45 degrees (from the zenith) : Geometrical Factor: ~ 1,040 cm^2sr (for electrons) : Thickness: 30 X_0, 1.3 λ_I

CHD/IMC

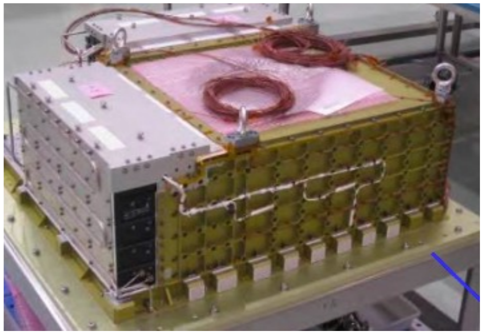

TASC

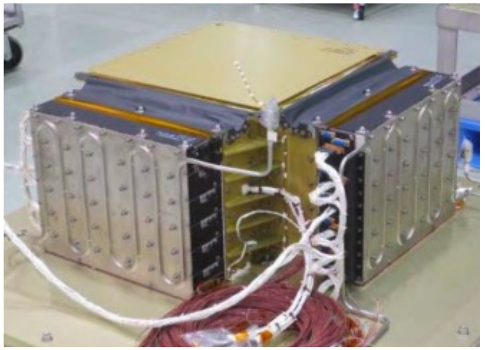

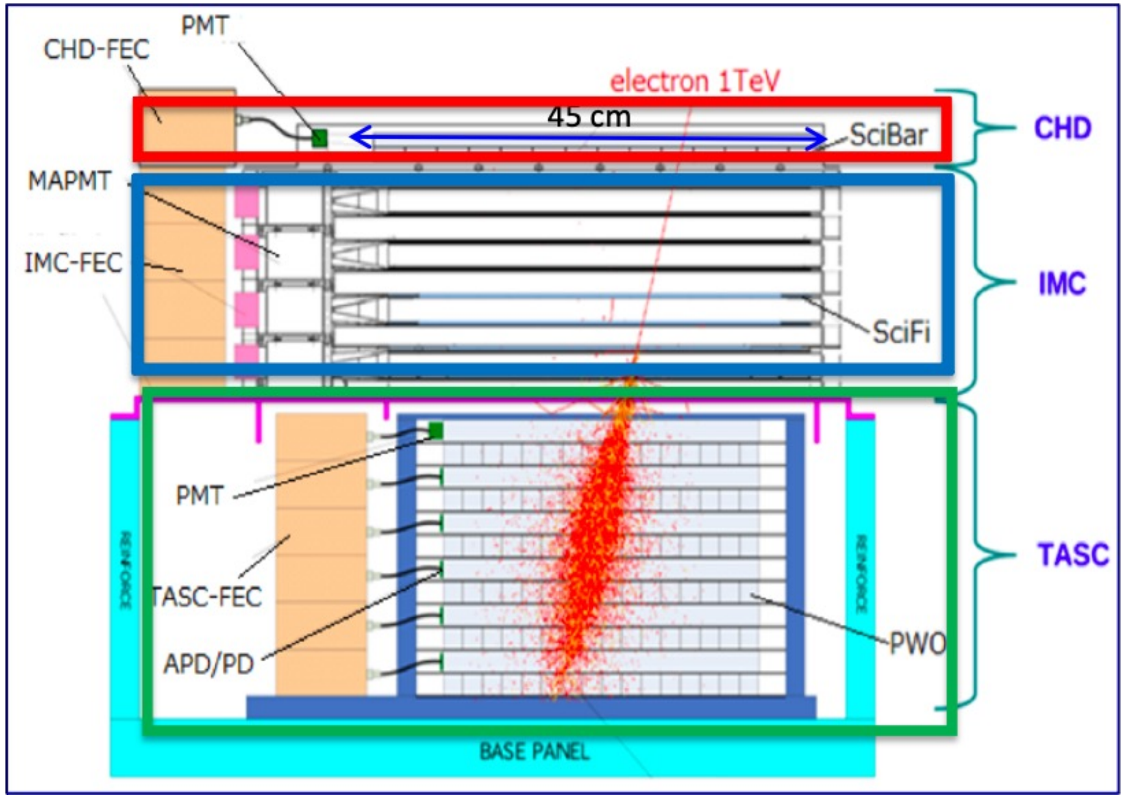

CHD – Charge Detector
- 2 layers x 14 plastic scintillating paddles
- **single element charge ID** from p to Fe and above (Z = 40)
- charge resolution ~0.1-0.3 e

IMC – Imaging Calorimeter
- Scifi. + tungsten absorbers: **3 X_0**
- 8 x 2 x 448 plastic scintillating fibers (1mm) **readout individually**
- **tracking** (~0.1° angular resolution) + **Shower imaging**

TASC – Total Absorption Calorimeter
- 6 x 2 x 16 lead tungstate ($PbWO_4$) logs: **27 X_0, 1.2 λ_I**
- **energy resolution:** ~2 % (>10GeV) for e , γ; ~30-35% for p, nuclei
- **e/p separation:** ~10^{-5}
- **angular resolution:** 0.2° for gamma-rays > ~50 GeV

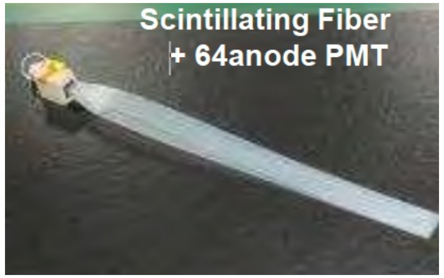

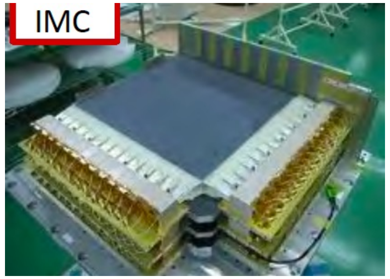

Examples of CALET Event Candidates

Electron, E=3.05 TeV

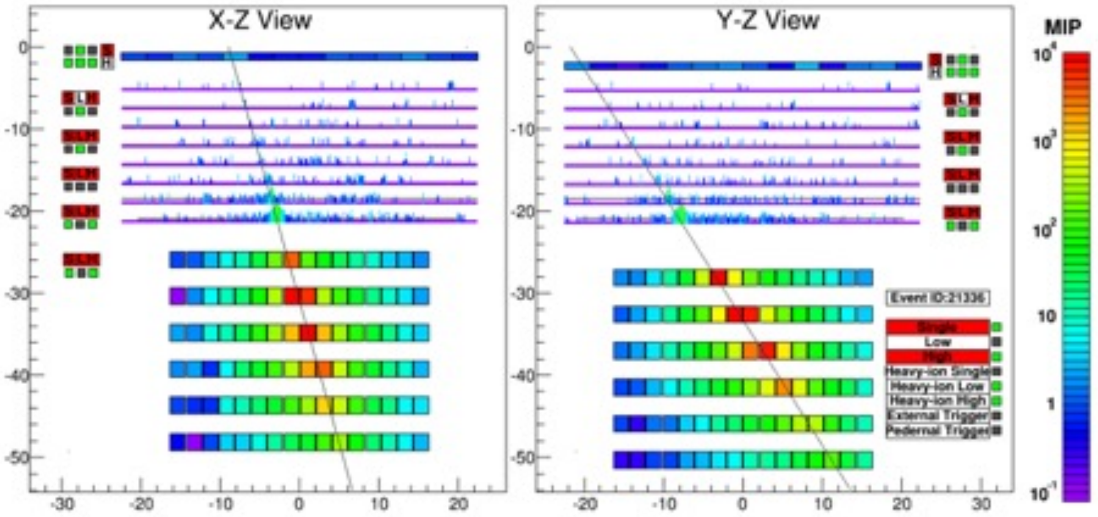

Proton, E_{TASC}=2.89 TeV

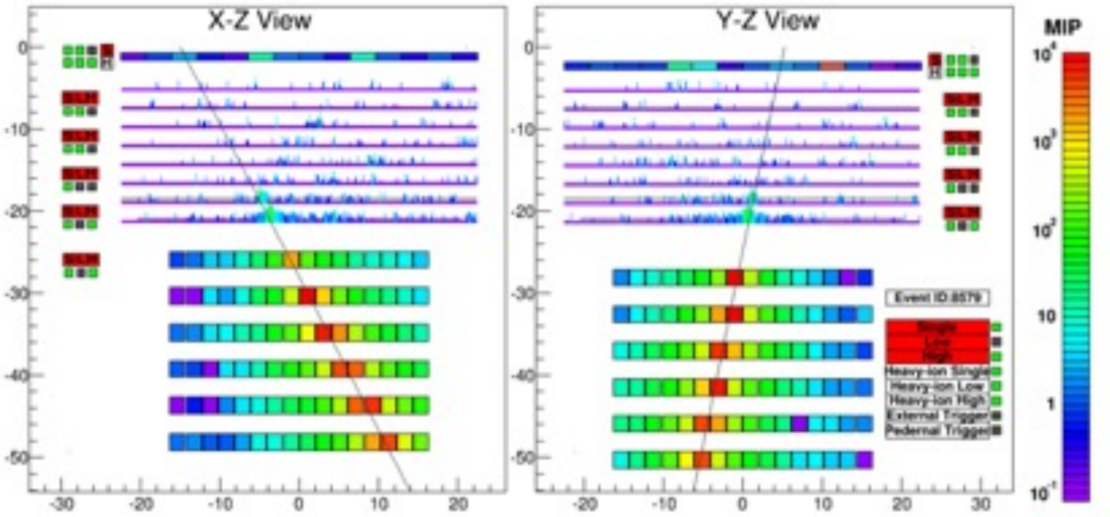

Gamma-ray, E=44.3 GeV

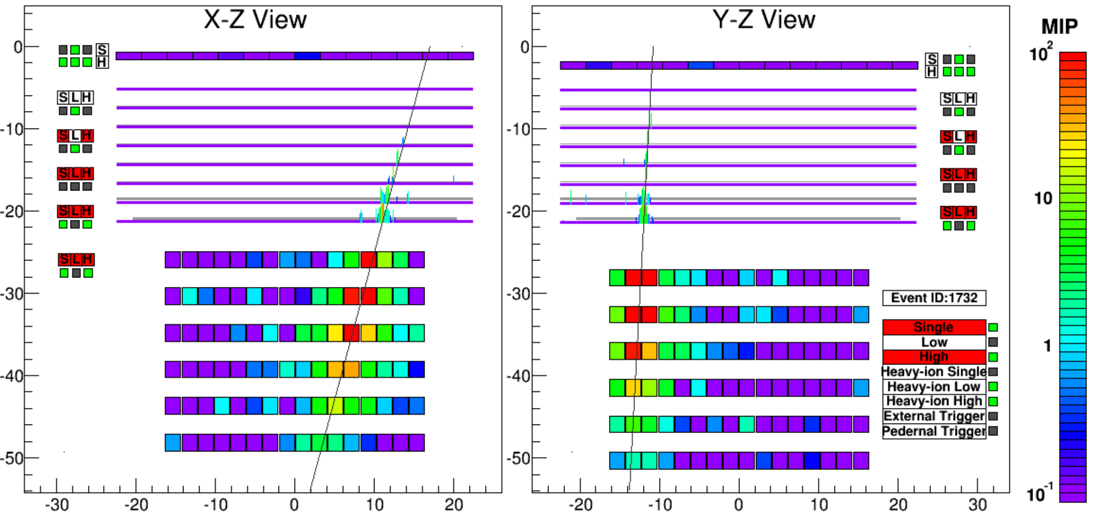

Iron, E_{TASC} =9.3 TeV

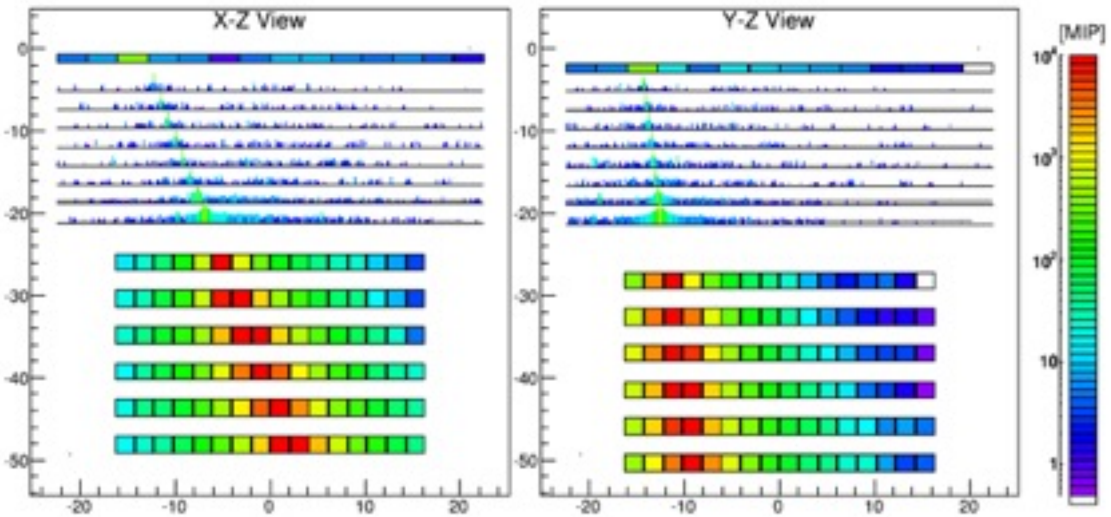

CALET Orbital Operations (during the first 8 years)

Geometrical Factor:
- 1040 cm^2 sr for electrons, light nuclei
- 1000 cm^2 sr for gamma-rays
- 4000 cm^2sr for ultra-heavy nuclei

High-energy(HE) trigger (> 10 GeV) statistics:
- Orbital operations : **2910 days (>8 years)** as of Sep. 30, 2023
- Observation time : 2.39×10^8 sec
- Live time fraction: ～ **86%**
- Exposure of HE trigger : ～**260 m^2 sr day**

Time duration of observation (day by day)

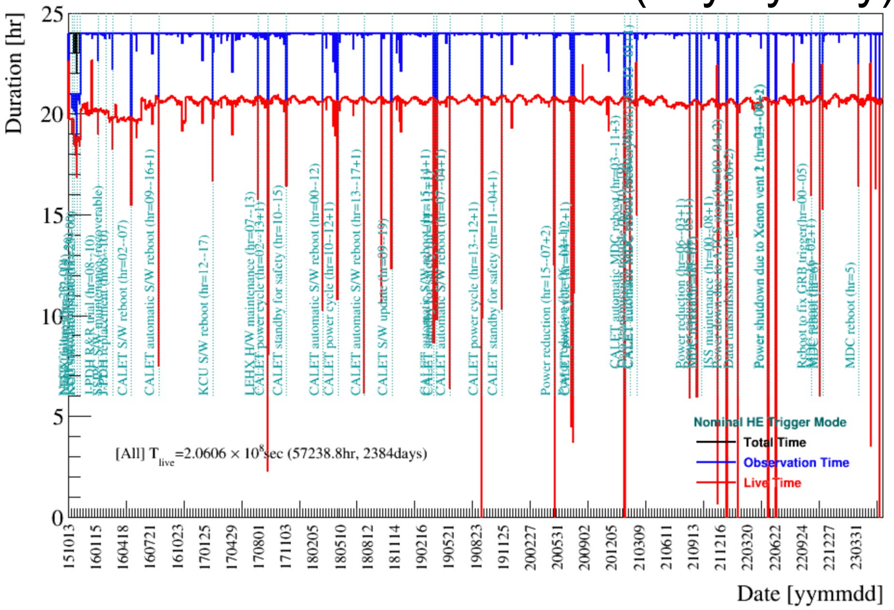

20.6 hours per day on average

Energy deposit (in TASC) spectrum: 1 GeV-1 PeV

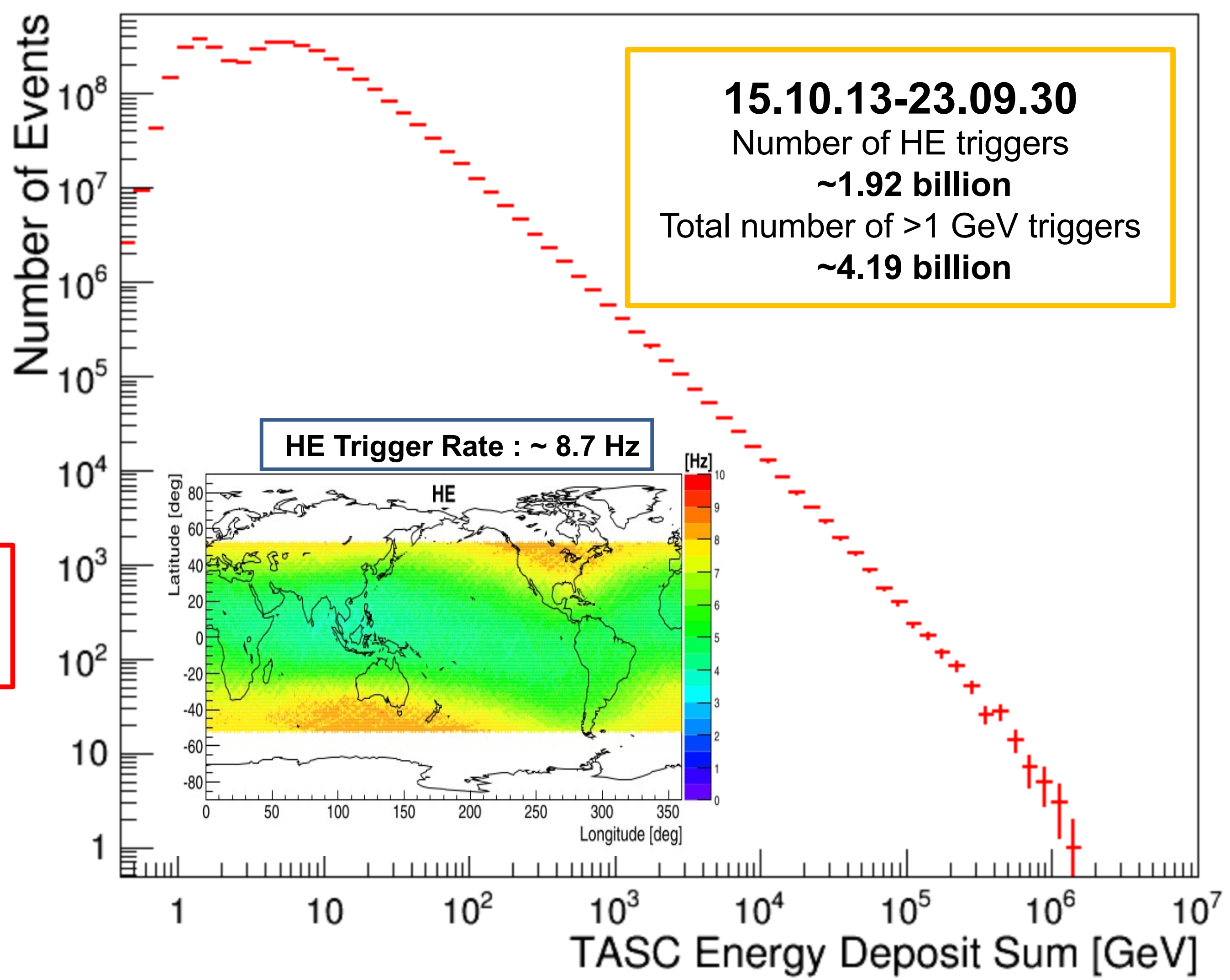

15.10.13-23.09.30
Number of HE triggers
~1.92 billion
Total number of >1 GeV triggers
~4.19 billion

HE Trigger Rate : ~ 8.7 Hz

Cosmic-ray All-electron Spectrum up to 7.5 TeV

to be published in PRL

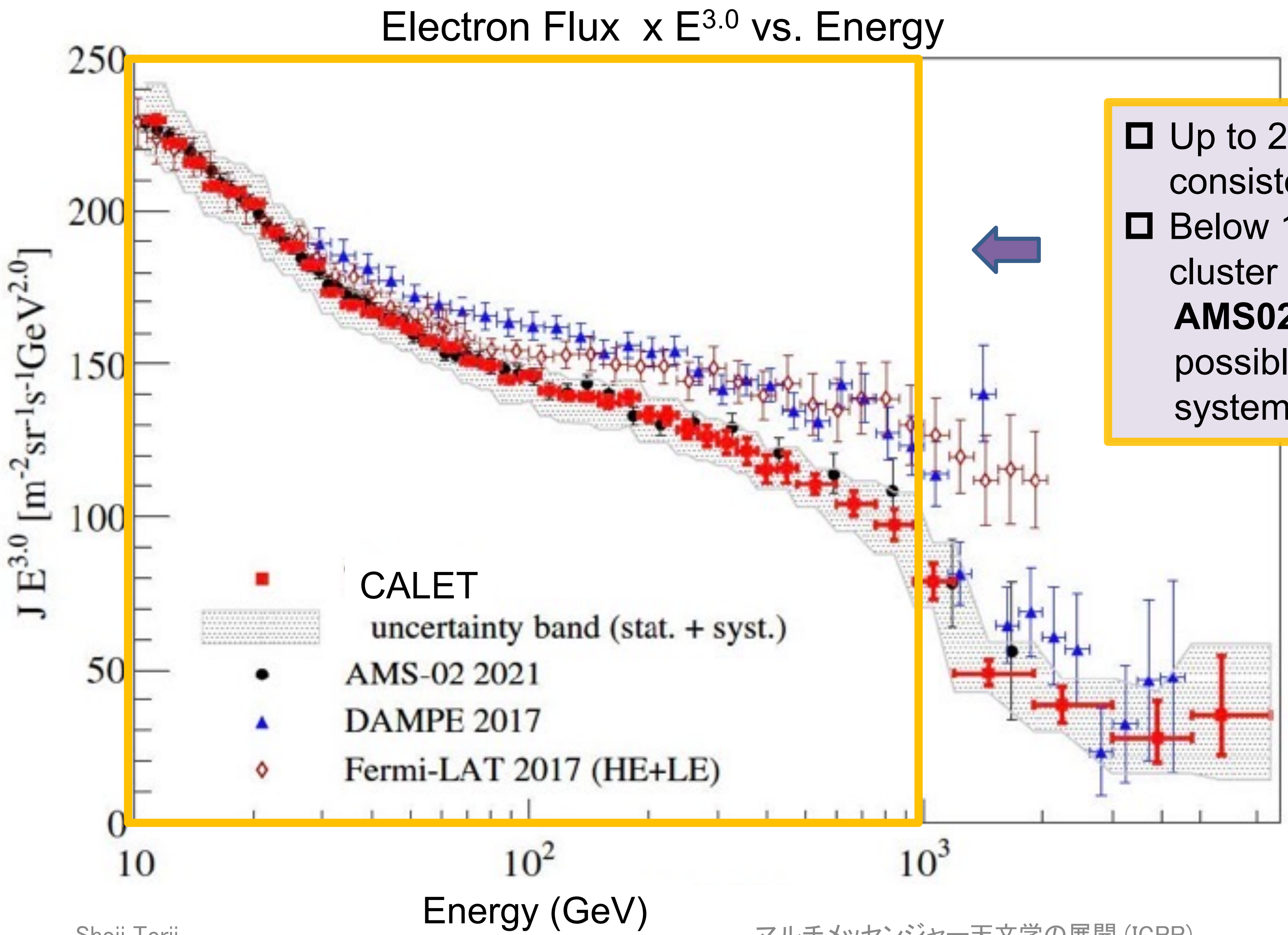

- Up to 2 TeV : CALET spectrum is consistent with AMS-02
- Below 1 TeV : Present measurements cluster into 2 groups:
  AMS02 + CALET and **FERMI + DAMPE** possibly indicating the presence of unkown systematics

The all-electron spectrum is **updated** using 2637 days of CALET observations:
Oct.13, 2015 – Dec. 31, 2022
7.02 million events > 10 GeV
to be published in PRL

Cosmic-ray All-electron Spectrum up to 7.5 TeV

Electron Flux x $E^{3.0}$ vs. Energy

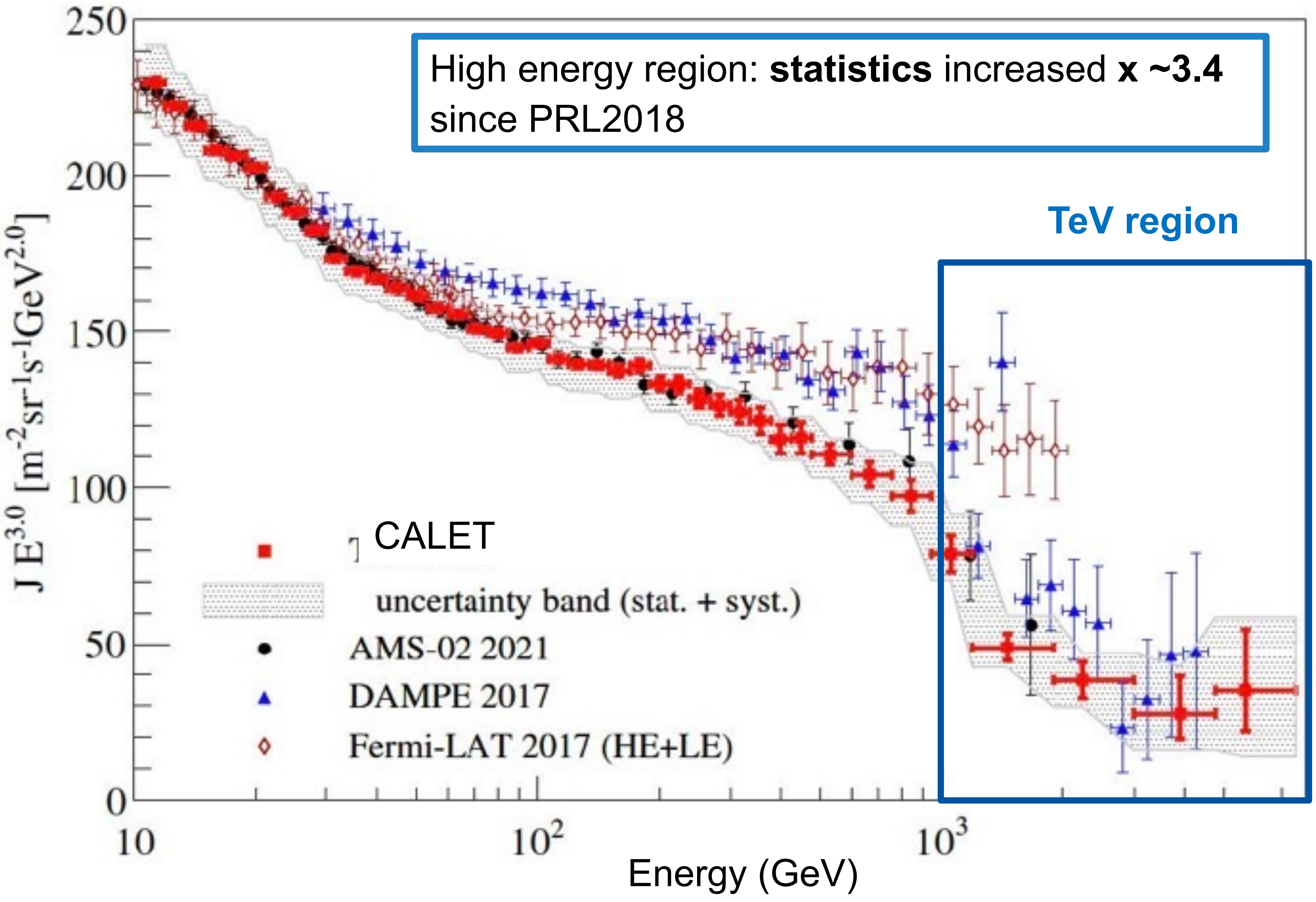

Energy loss due to Synchrotron and Inverse Compton : $dE/dt = -bE^2$

⇨ Observable sources of the electrons in the TeV region should be located at a distance < ~1 kpc and produced at a year < ~10^5 yr.

⇨ **Softening of the spectrum is expected above 1 TeV** since only a few SNRs are observed to keep this condition.

CALET observes a flux suppression above 1 TeV with a **significance > 6 σ**, a considerable improvement with respect to the result published in PRL2018 (~4 σ).

Advanced analysis is going on for electron identification above 5 TeV.

Towards an Interpretation of the CALET All-electron Spectrum

Tentative spectral fits of the CALET all-electron spectrum in 10 GeV-7.5 TeV including pulsars and a possible Vela SNR contribution:

- The positron flux of AMS-02 is shown with expected contributions (red line) from secondaries (red dashed line) and sum of several pulsars (red dotted line).
- The electron flux is shown with contribution from by secondaries + distant SNRs (black dashed line) and the Vela SNR (green line).
- The fitted model includes a possible contribution from the Vela SNR , consistent with an energy output of 0.7 x 10^{48} erg in electron CR above 1 GeV.

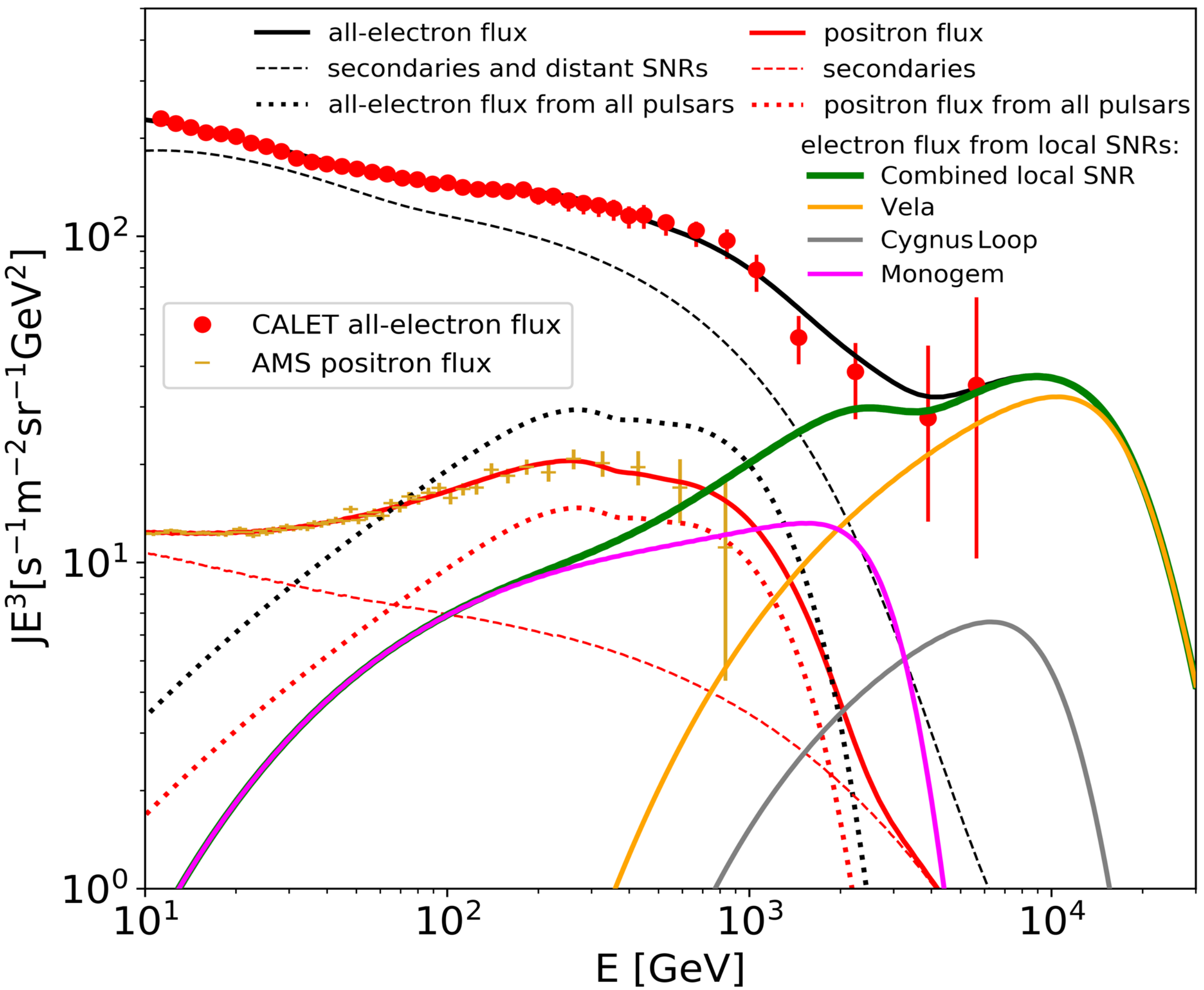

Cosmic-ray Proton Spectrum

PRL 129 101102 (2022)

Flux x $E^{2.7}$ vs. Kinetic energy [Oct.2015- Apr.2023]

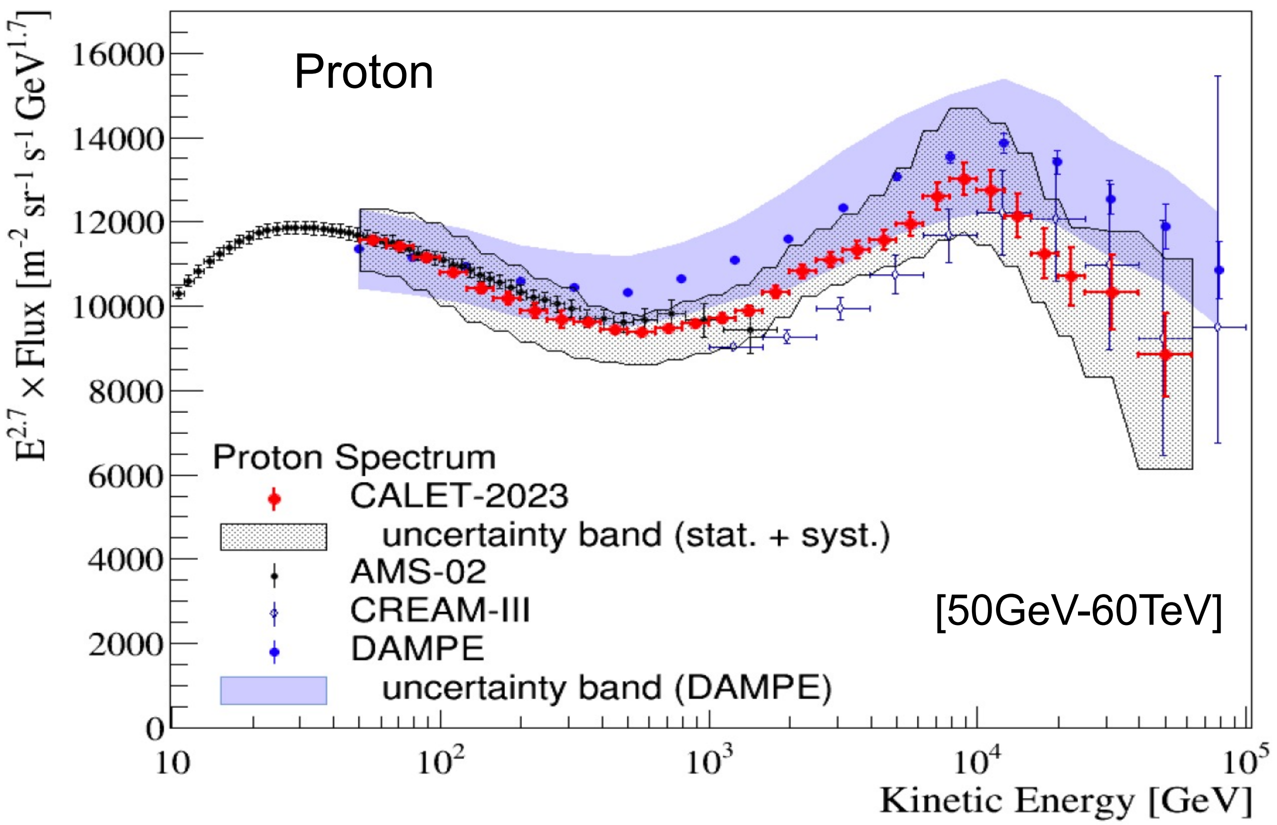

Fitting by DBPL Function

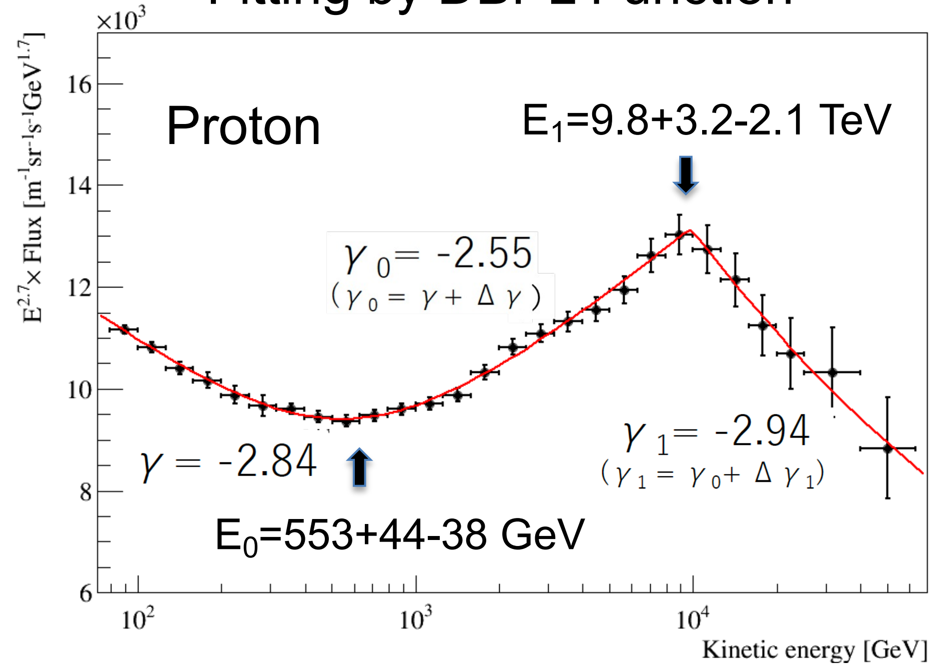

Energy dependence of power index

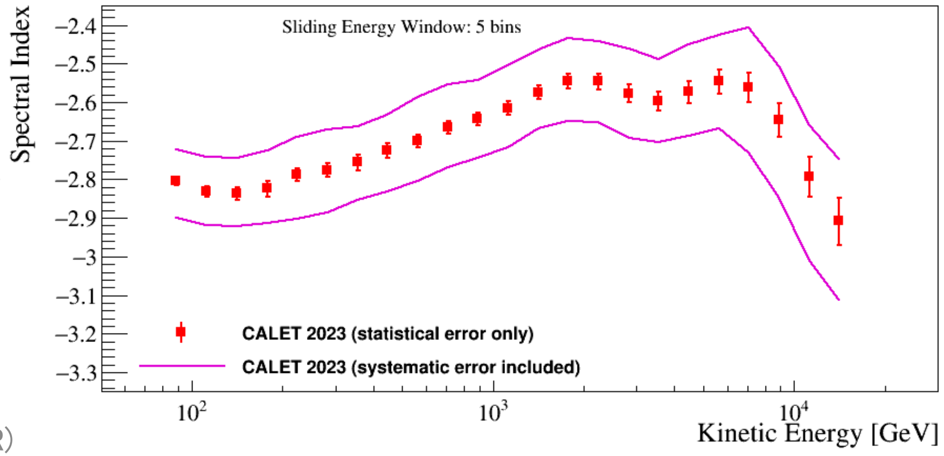

Double Power Law Function: HARDENING SOFTENING

$$\Phi(E) = C \times \left(\frac{E}{1\ \mathrm{GeV}}\right)^{\gamma} \times \left[1 + \left(\frac{E}{E_0}\right)^{s}\right]^{\frac{\Delta\gamma}{s}} \times \left[1 + \left(\frac{E}{E_1}\right)^{s_1}\right]^{\frac{\Delta\gamma_1}{s_1}}$$

Cosmic-ray Helium Spectrum

PRL 130 171002 (2023)

Flux x $E^{2.6}$ vs. Kinetic energy [Oct. 2015 - Apr. 2022]

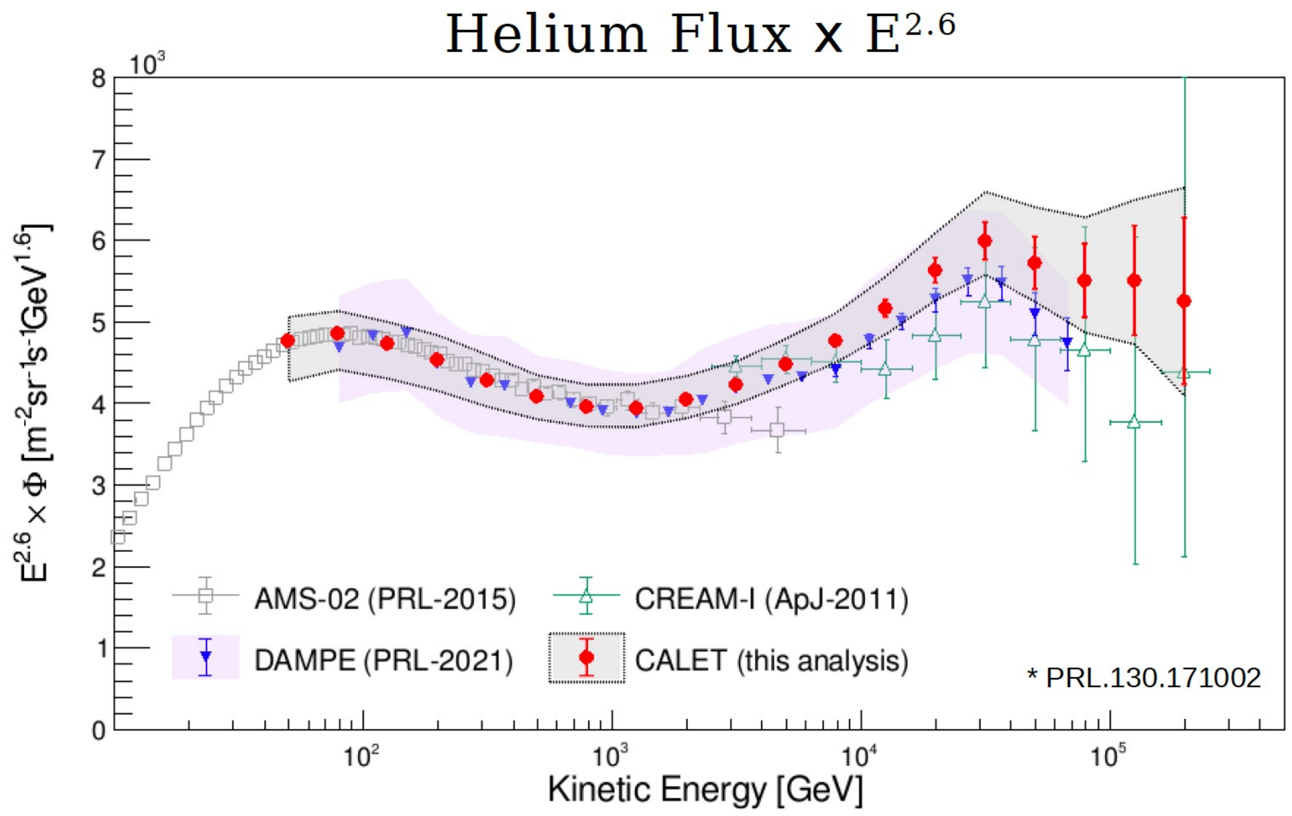

Fitting by Double Power Law (DBPL) function

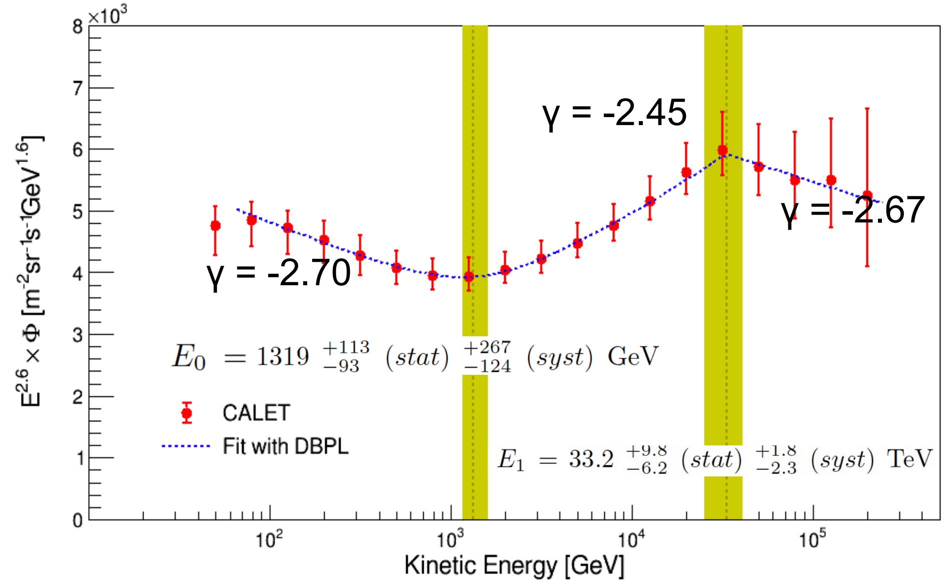

Energy dependence of power index

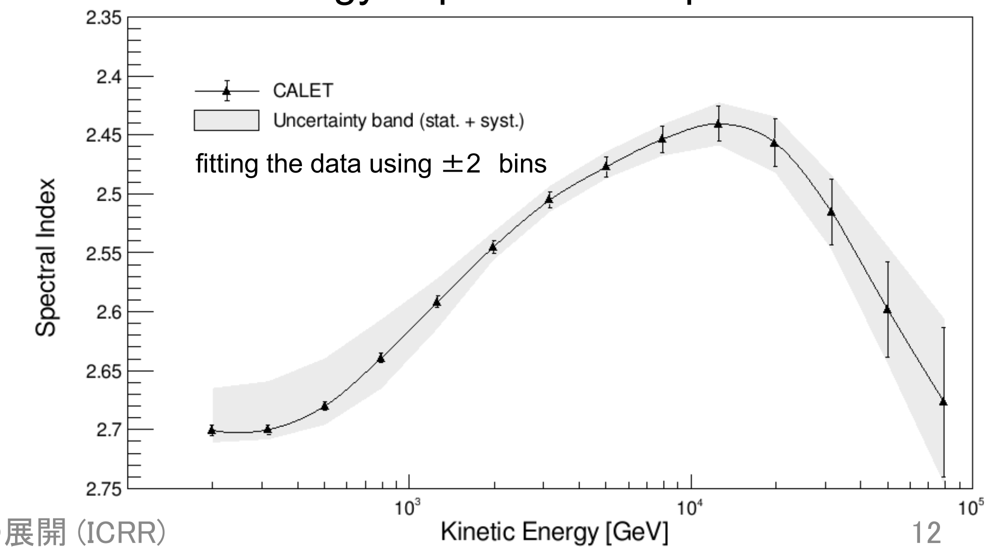

Double Power Law Function: HARDENING SOFTENING

$$\Phi(E) = C\left(\frac{E}{GeV}\right)^{\gamma}\left[1+\left(\frac{E}{E_0}\right)^{S}\right]^{\frac{\Delta\gamma}{S}}\left[1+\left(\frac{E}{E_1}\right)^{S_1}\right]^{\frac{\Delta\gamma_1}{S_1}}$$

Comparison of Proton and Helium Spectrum

Proton & Helium Spectrum vs Energy/nucleon

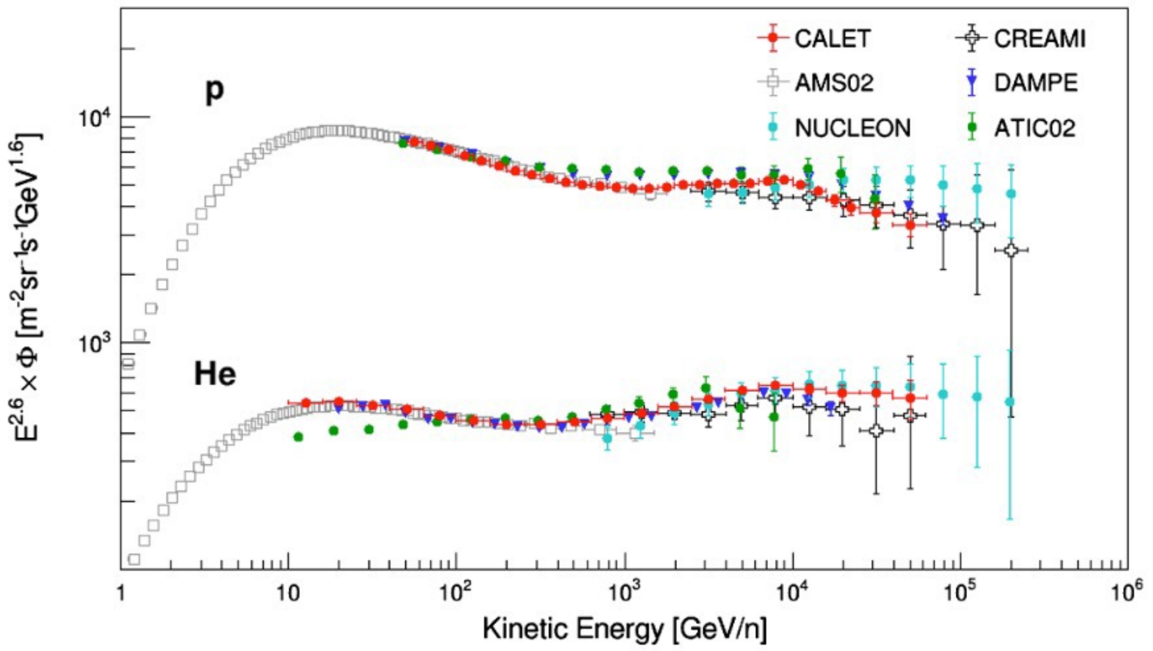

Proton & Helium Spectrum vs Rigidiy

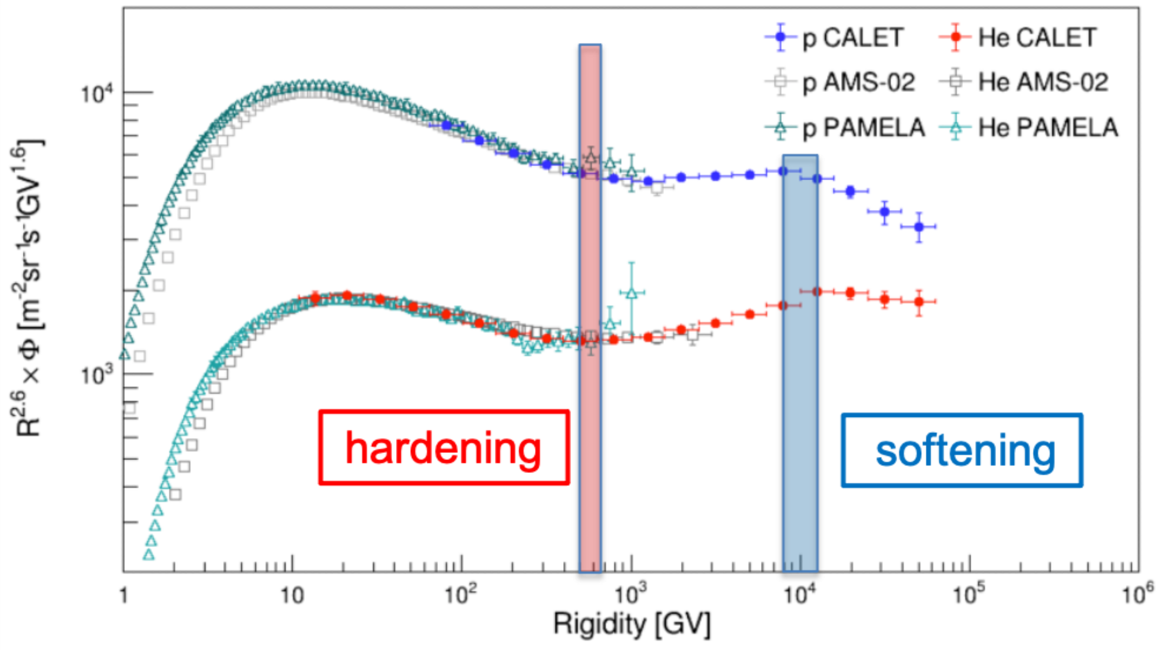

- Both of proton and helium spectrum present a similar structure of hardening and softening.
- The softening of p & He spectrum around 10 TV indicates a possible limit of the acceleration.

Best fit parameters with DBPL function for proton and helium spectrum (energy/particle)

	γ	E_0 (GeV)	$\Delta\gamma$	S	E_1 (TeV)	$\Delta\gamma_1$	S_1
Proton	-2.843 ±0.005	553^{+44}_{-38}	0.29 ±0.01	2.1 ± 0.4	$9.8^{+3.2}_{-2.1}$	$-0.39^{+0.15}_{-0.18}$	~ 90
Helium	$-2.703^{+0.005}_{-0.006}$	1319^{+113}_{-93}	$0.25^{+0.02}_{-0.01}$	$2.7^{+0.6}_{-0.5}$	$33.2^{+9.8}_{-6.2}$	$-0.22^{+0.07}_{-0.10}$	30

Observations of Cosmic-ray Nuclei from C to Ni

Preliminary spectra of Carbon – Iron

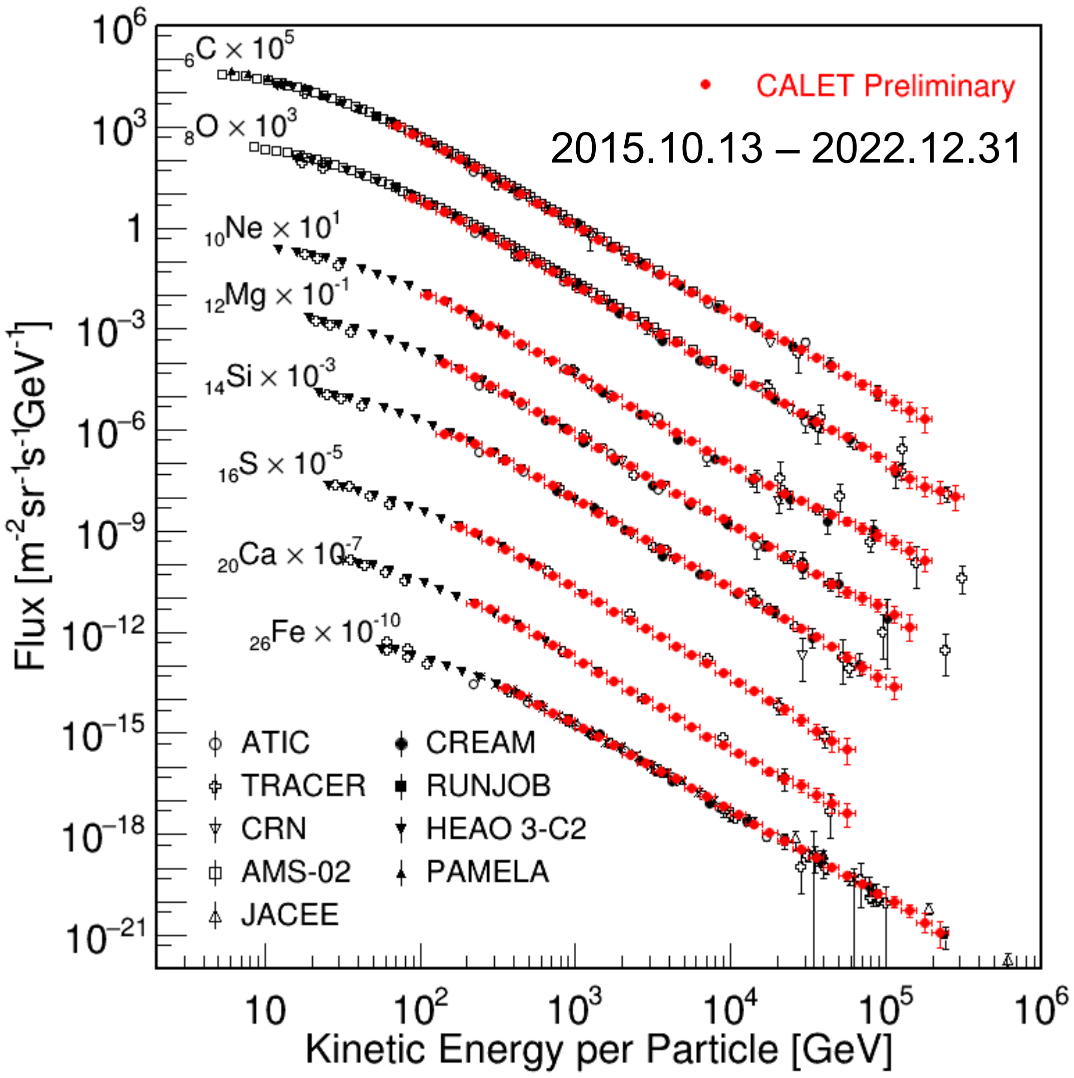

With excellent charge-ID of individual elements CALET is exploring the Table of Elements in the multi-TeV domain

Charge distribution from Proton to Nickel
(periodic table of elements by CALET)

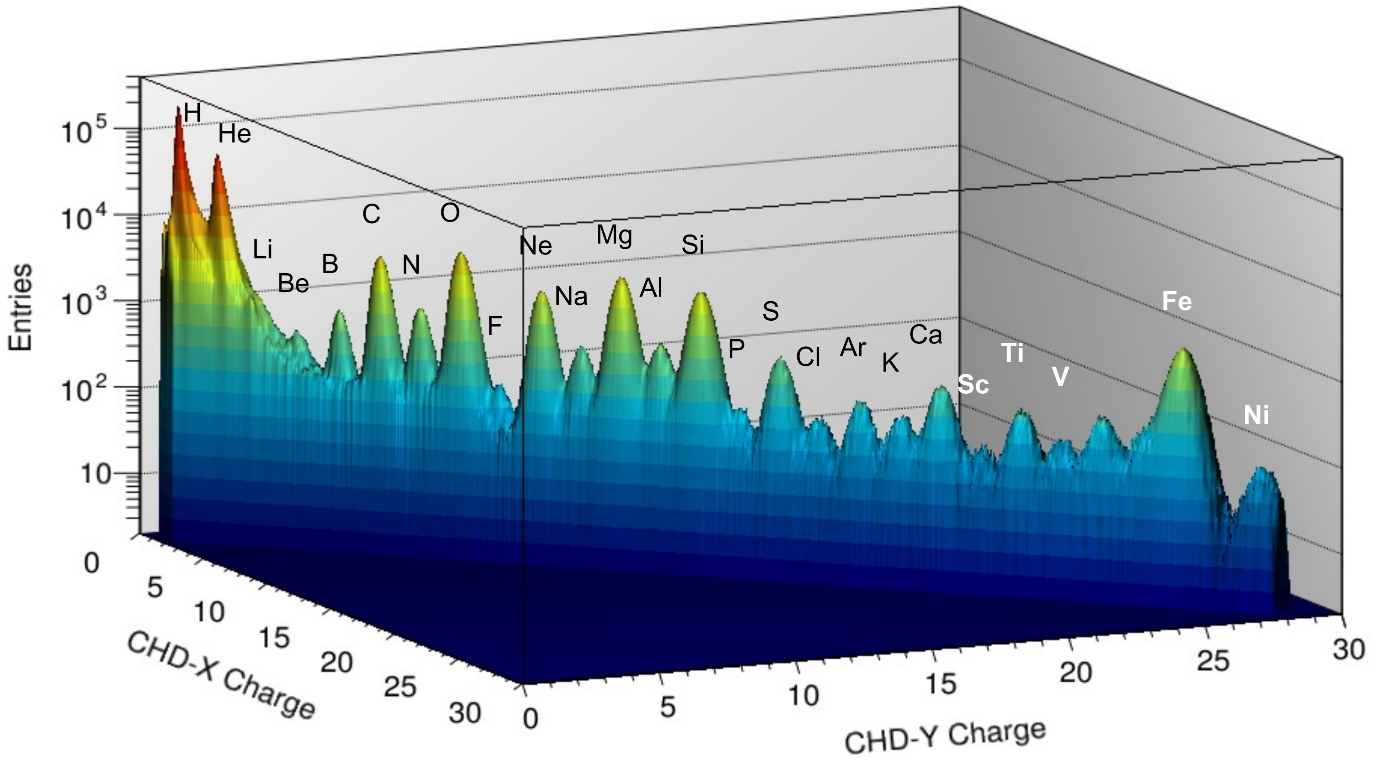

Carbon, Oxygen and Boron Energy Spectra

PRL 125 251102 (2020)
PRL 129 251103 (2022)

Flux x $E^{2.7}$ vs kinetic energy per nucleon [8.4 GeV- 3.8 TeV]

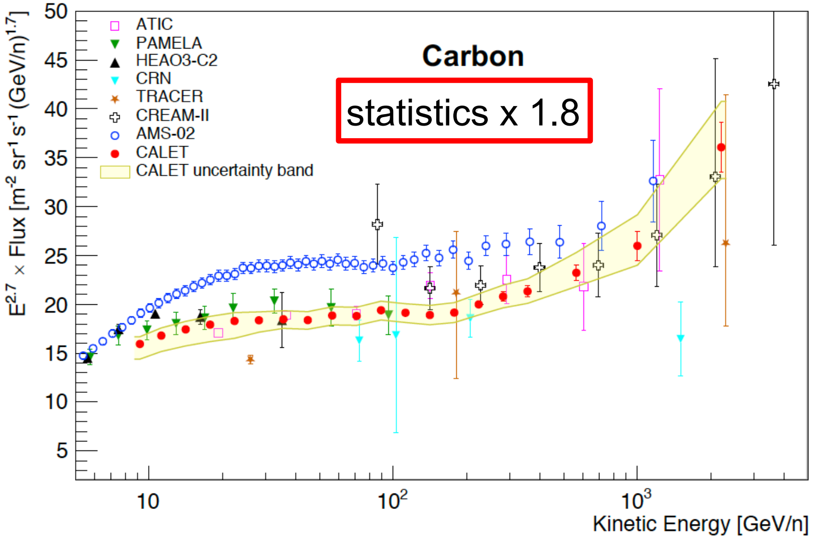

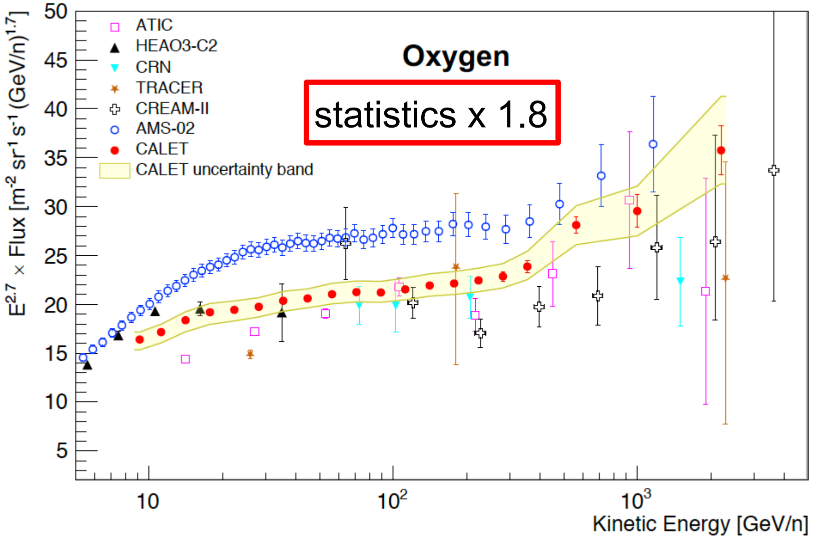

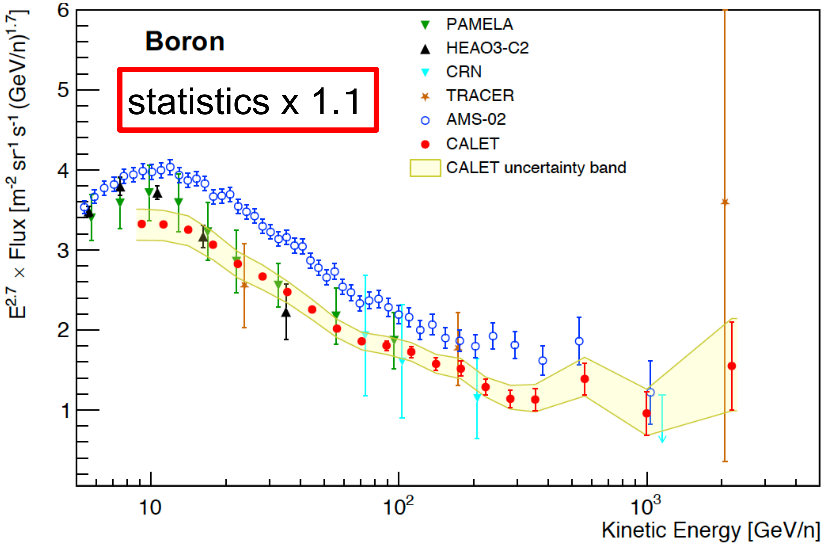

Fitting with double power law function

$$\Phi(E) = \begin{cases} c\left(\frac{E}{\mathrm{GeV}}\right)^{\gamma} & E \le E_0 \\ c\left(\frac{E}{\mathrm{GeV}}\right)^{\gamma}\left(\frac{E}{E_0}\right)^{\Delta\gamma} & E > E_0 \end{cases}$$

C-O fit

$\gamma = -2.66 \pm 0.02$
$E_0 = (260 \pm 50)$ GeV/n
$\Delta\gamma = 0.19 \pm 0.04$
$\chi^2/\mathrm{dof} = 23/25$

B fit

$\gamma = -3.03 \pm 0.03$
E_0 fixed from C-O
$\Delta\gamma = 0.32 \pm 0.14$
$\chi^2/\mathrm{dof} = 5.2/11$

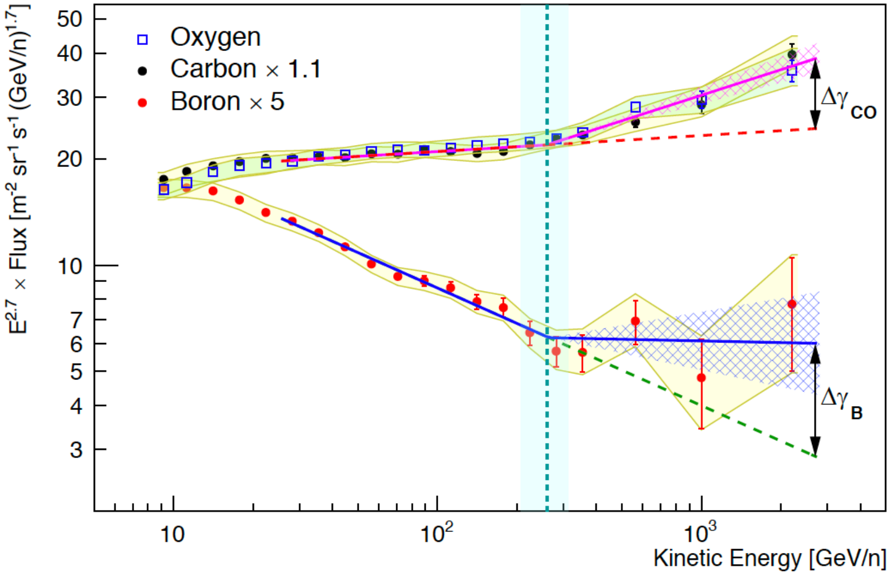

- C and O fluxes harden in a similar way above 200 GeV/n.
- B spectrum clearly different from C-O as expected for primary and secondary CR.
- The flux hardens more for B than for C and O above 200 GeV/n, albeit with low statistical significance.

B/C, B/O and C/O Flux Ratio

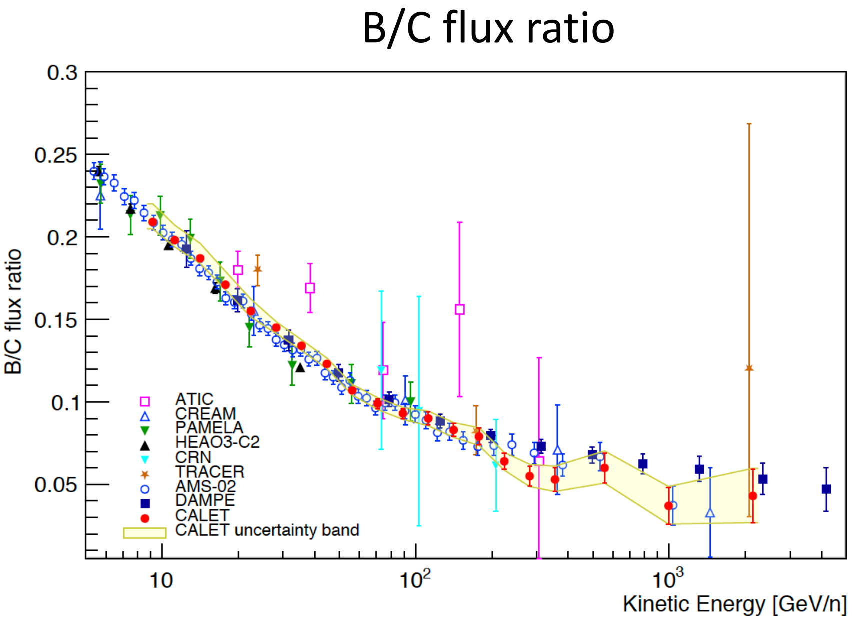

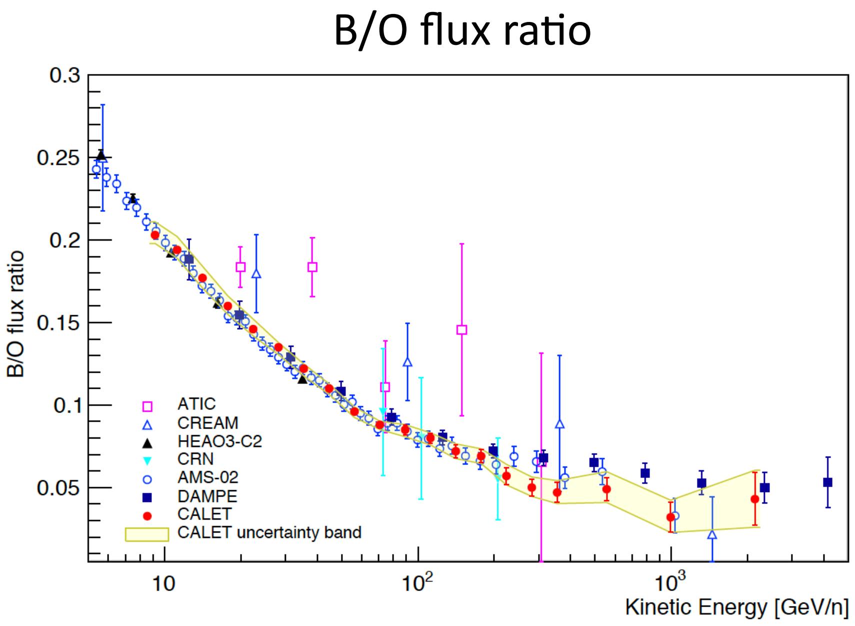

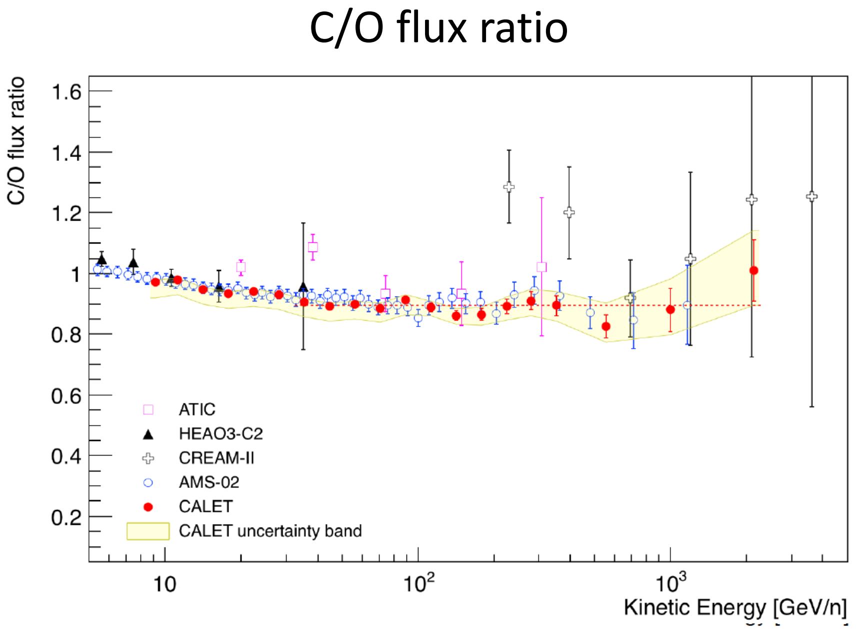

- Flux ratios of B/C and B/O are in agreement with AMS02 and lower than DAMPE result above 300 GeV/n, although consistent within the error bars.
- C/O flux ratio as a function of energy is in good agreement with AMS-02.
- At E > 30 GeV/n the C/O ratio is well fitted to a constant value 0.90±0.03 with χ^2/dof = 8.1/13.
  ⇨ C and O fluxes have the same energy dependence.
- At E < 30 GeV/n C/O ratio is slightly softer.
  ⇨ secondary C from O and heavier nuclei spallation

Spectral Fit of B/C and B/O

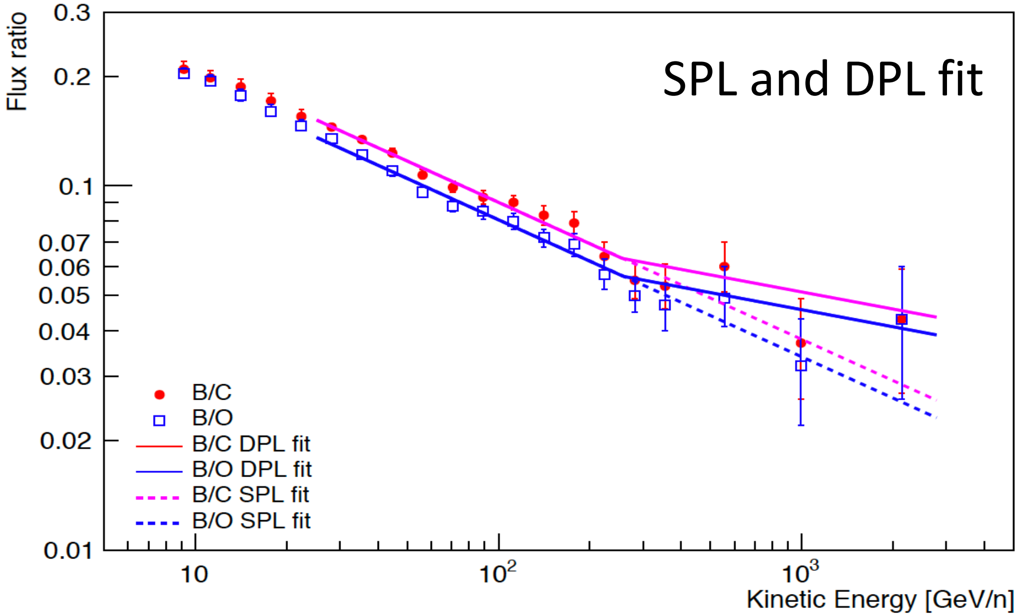

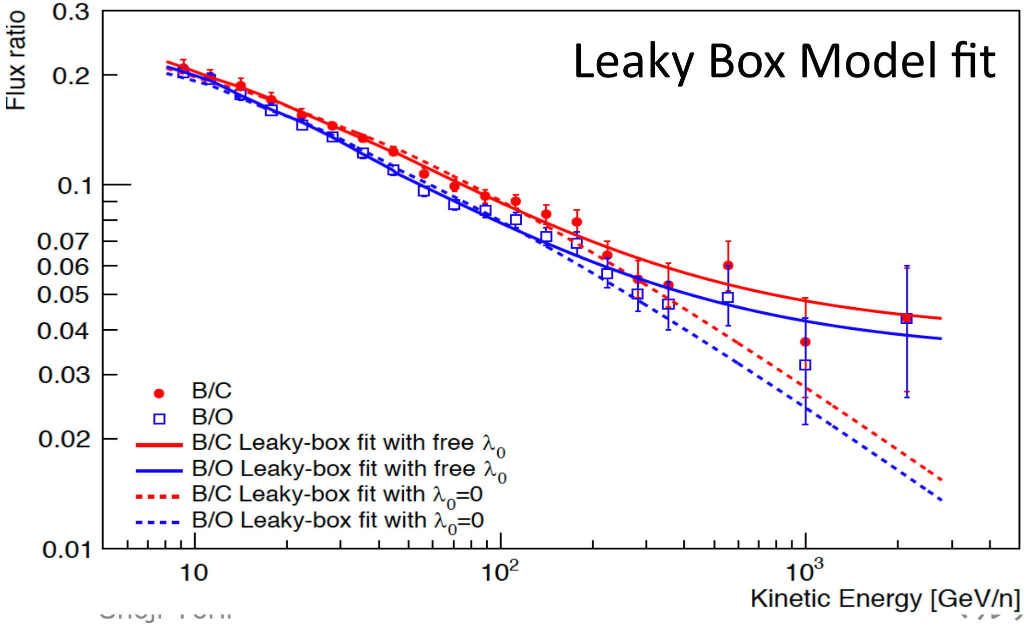

Simultaneous fit to B/C and B/O (E>25 GeV/n) with same parameters except normalization

SPL fit	$\Gamma = -0.376 \pm 0.014$	(χ^2/dof = 19/27)
DPL fit	$\Delta\Gamma = 0.22 \pm 0.10$	(χ^2/dof = 15/26)

Leaky-box model fit [ApJ **752** 69 (2012)]

$$\frac{\Phi_B(E)}{\Phi_C(E)} = \frac{\lambda(E)\lambda_B}{\lambda(E)+\lambda_B}\left[\frac{1}{\lambda_{C\to B}} + \frac{\Phi_O(E)}{\Phi_C(E)}\frac{1}{\lambda_{O\to B}}\right] \quad \frac{\Phi_B(E)}{\Phi_O(E)} = \frac{\lambda(E)\lambda_B}{\lambda(E)+\lambda_B}\left[\frac{1}{\lambda_{O\to B}} + \frac{\Phi_C(E)}{\Phi_O(E)}\frac{1}{\lambda_{C\to B}}\right]$$

$\lambda(E)$: mean escape path length

$$\lambda(E) = kE^{-\delta} + \lambda_0$$

λ_0 : residual path length

δ : diffusion coefficient spectral index

Fit parameters	λ_0 =0 fixed	λ_0 free
k (g/cm^2))	13.1 ± 0.2	13.0 ± 0.3
δ	0.61 ± 0.01	0.81 ± 0.04
λ_0 (g/cm^2)	0	1.17 ± 0.16
χ^2/dof	58.3/38	17.9/37

Significance of $\lambda_0 \neq 0$ > 5σ
⇨ Residual path length could explain the flattening of B/C, B/O ratios at high energies.

Cosmic-ray Iron Energy Spectrum

PRL 126 241101 (2022)

Flux x $E^{2.6}$ vs kinetic energy per nucleon (Nov.2016-Dec.2022)

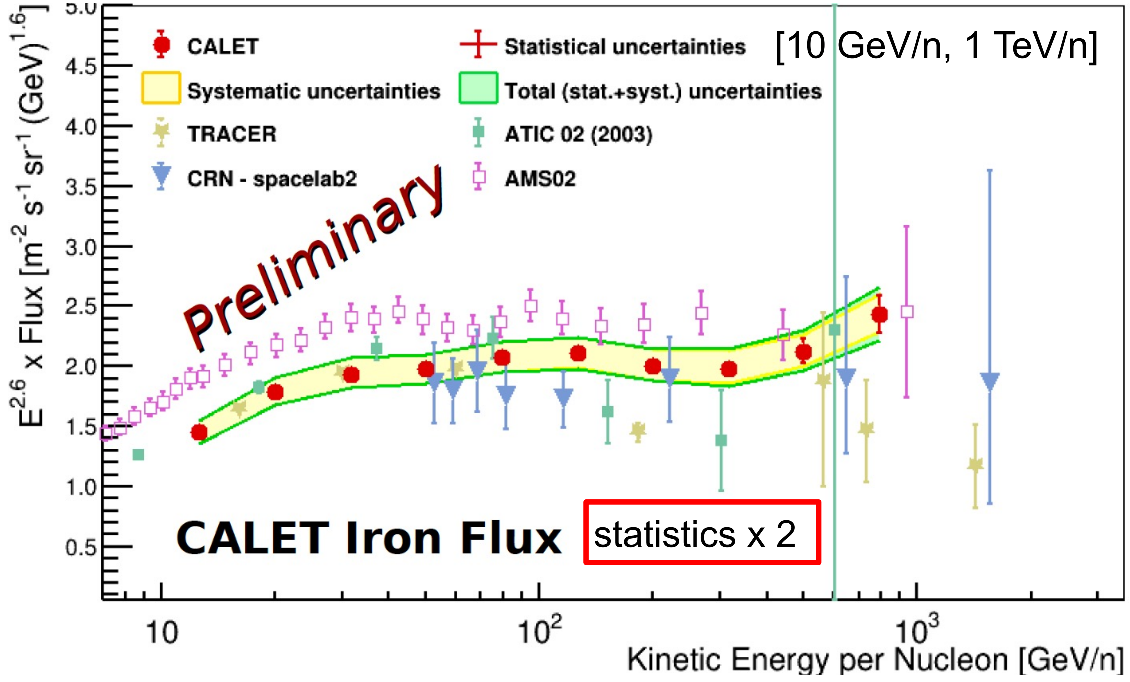

Fit from 50 to 800 GeV/n, with SPL & DPL

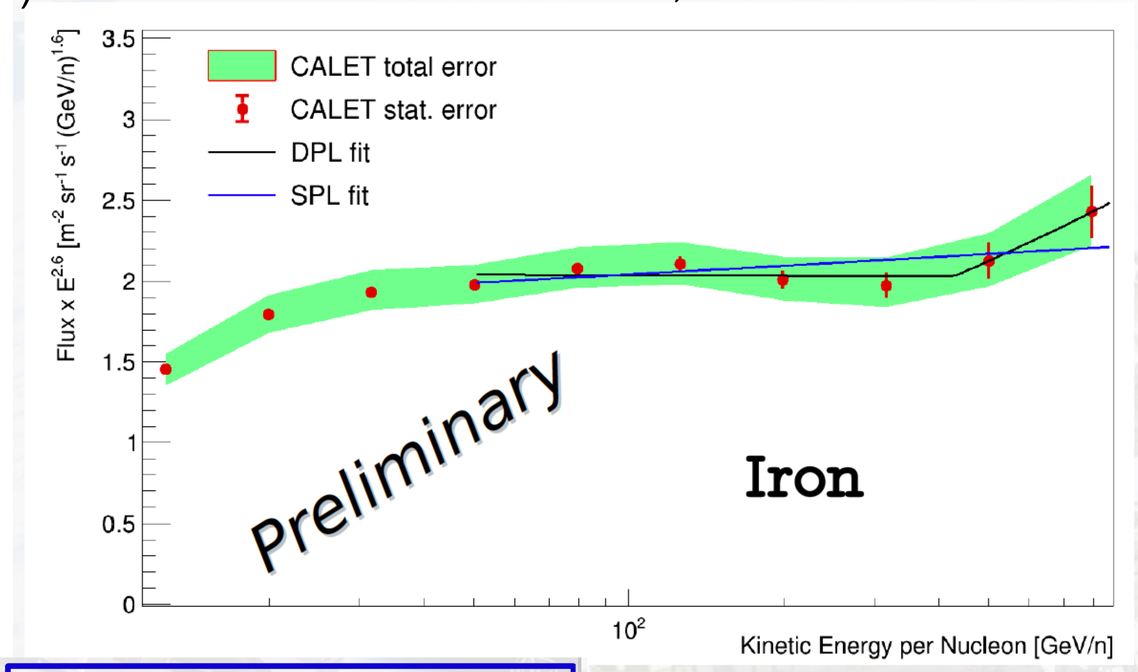

Low energy (< 10 GeV) measurement using geomagnetic cut-off (Oct. 2015 to May 2021)

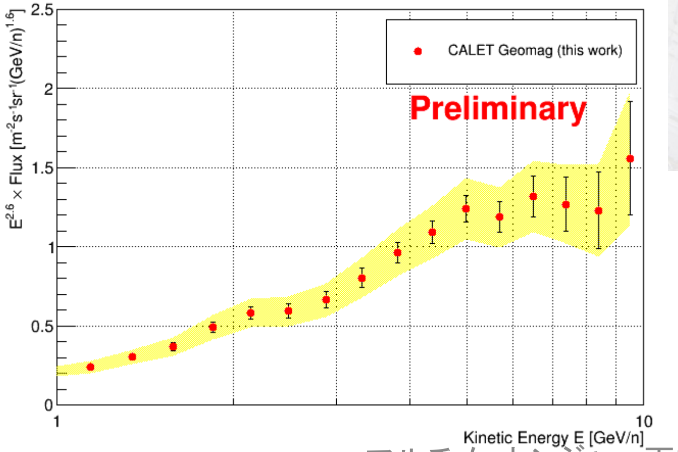

SPL Fit

$$\Phi(E) = C\left(\frac{E}{1\ \mathrm{GeV}}\right)^{\gamma}$$

- $\gamma = -2.56 \pm 0.01(\mathrm{stat}) \pm 0.03(\mathrm{sys})$
- $\chi^2/\mathrm{DOF} = 2.7/5$

The significance of the fit with the DPL in the studied energy range is not sufficient to exclude the possibility of a single power law.

DPL Fit

$$\Phi(E) = \begin{cases} c\left(\frac{E}{\mathrm{GeV}}\right)^{\gamma} & E \le E_0 \\ c\left(\frac{E}{\mathrm{GeV}}\right)^{\gamma}\left(\frac{E}{E_0}\right)^{\Delta\gamma} & E > E_0 \end{cases}$$

- $\gamma = -2.60 \pm 0.01(\mathrm{stat}) \pm 0.08(\mathrm{sys})$
- $\chi^2/\mathrm{DOF} = 0.8/3$
- $\Delta\gamma = 0.29 \pm 0.27$
- $E_0 = (428 \pm 314)$ Gev/n

Cosmic-ray Nickel Energy Spectrum

PRL 128 131103 (2022)

Flux x $E^{2.6}$ vs kinetic energy per nucleon

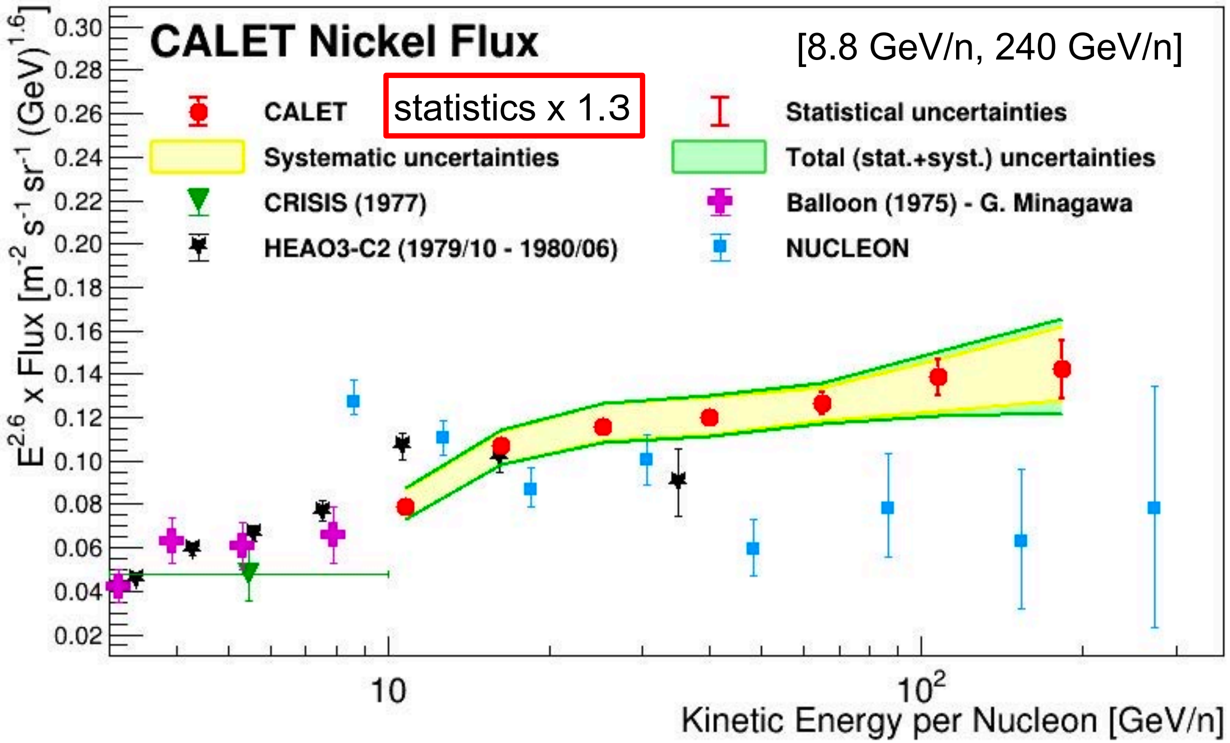

Fit from 20 to 240 GeV/n, with a SPL

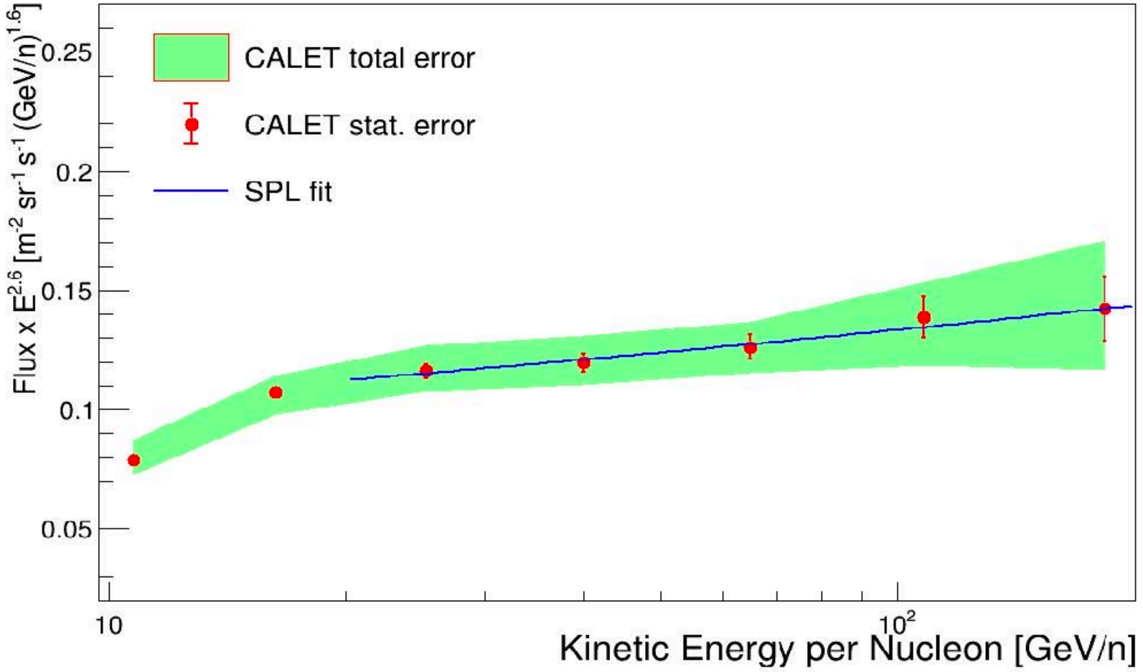

Charge separation between Fe and Ni

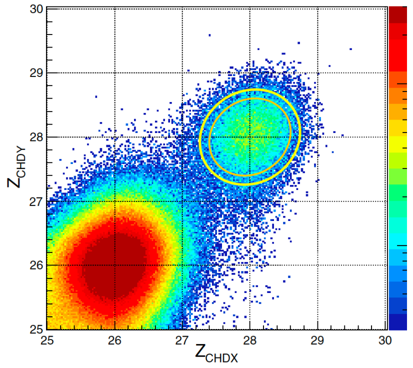

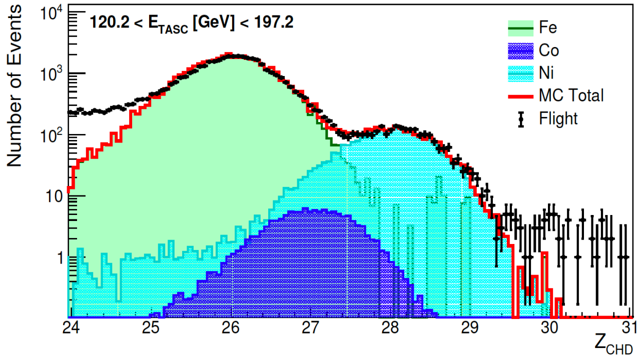

SPL Fit

$$\Phi(E) = C\left(\frac{E}{1\ \mathrm{GeV}}\right)^{\gamma}$$

- $\gamma = -2.49 \pm 0.03(\mathrm{stat}) \pm 0.07(\mathrm{sys})$
- $\chi^2/\mathrm{DOF} = 0.1/3$

From 20 to 240 GeV/n the nickel flux is consistent with the hypothesis of an SPL Spectrum.

Flux Ratio of Primary Elements

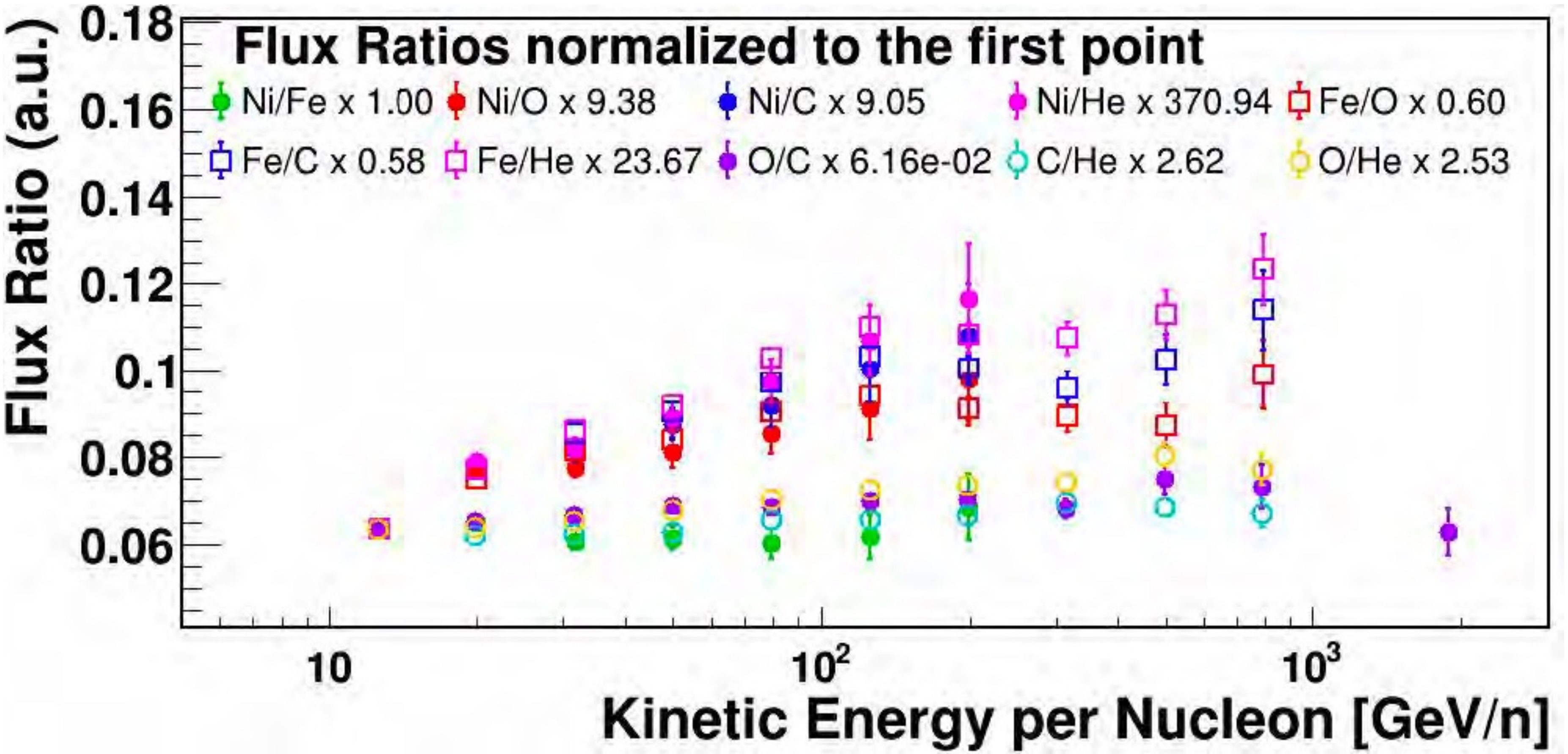

- All the ratios are compatible with a constant value above 100 GeV/n (Ni/Fe is constant starting from 10 GeV/n) .
- Whereas at low energy, the ratio increases in a similar way for Ni/O, Ni/C, Ni/He, Fe/O, Fe/C, Fe/He.
- The increment at low energy is less pronounced for O/C, O/He and C/He.

Ultra-heavy Cosmic-ray Nuclei (26 < Z ≤ 44)

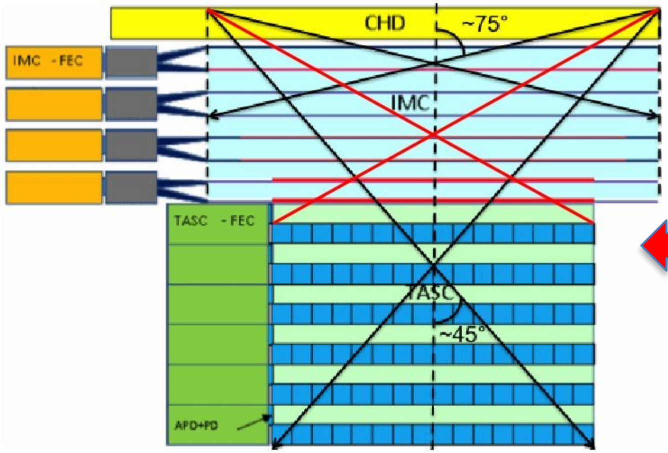

- A special UH CR trigger uses the CHD and the first 4 layers of the IMC to achieve an expanded x 4 geometric factor **GF ~ 4400 cm^2 sr** without energy information**.**
  (~260 million events)
- A subset of events pass through the top of the TASC (~65 million events) with energy information,

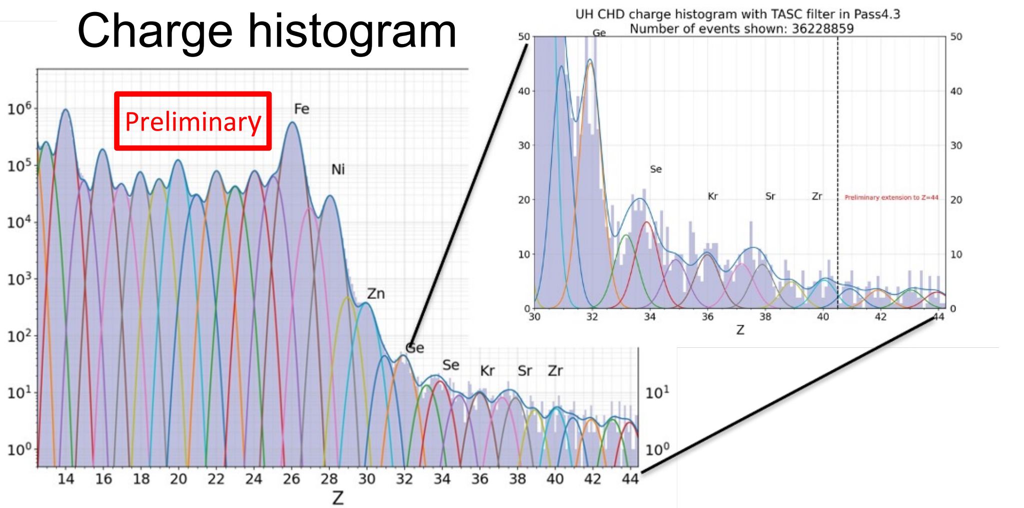

Mesurement of the relative abundances of the elements above Fe through $_{44}$Ru (Fe =1)

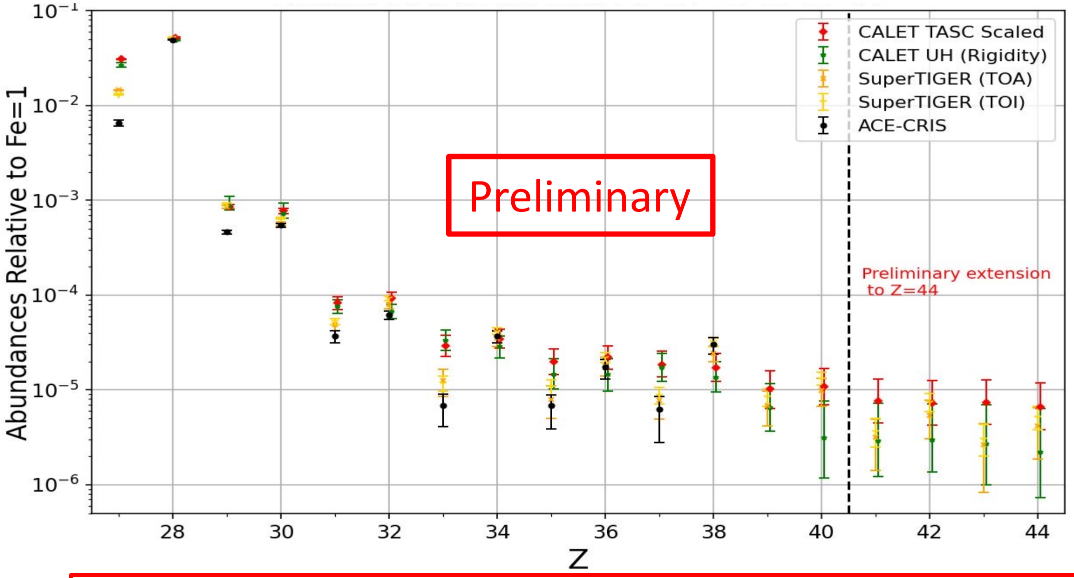

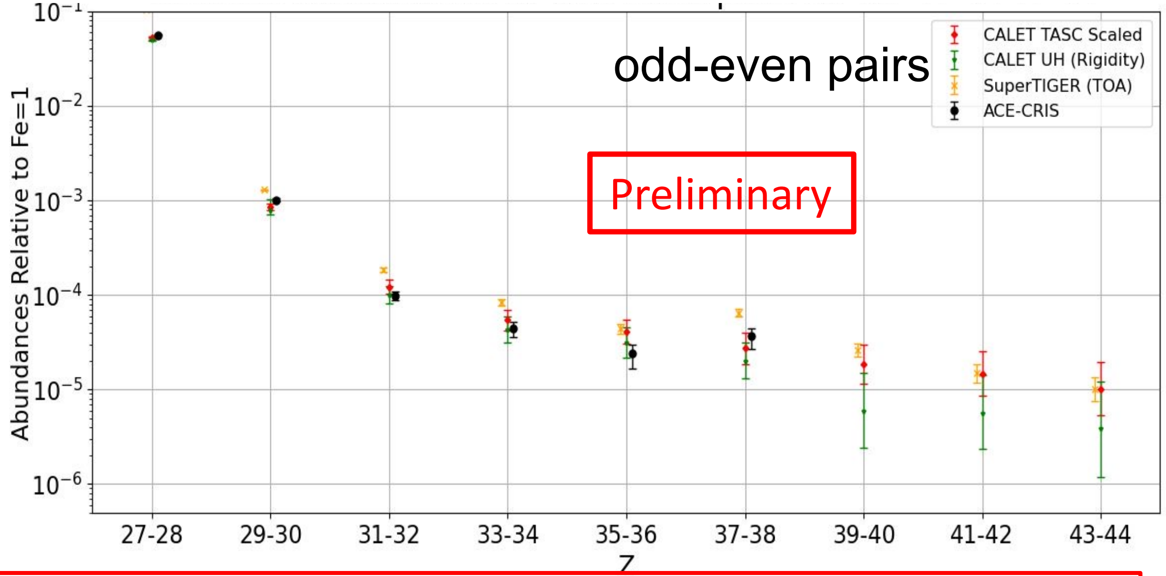

The CALET UH element ratios relative to Fe are consistent with Super-TIGER and ACE abundances.

CALET γ–ray Sky Map and Energy Spectra

- Effective area: ~400 cm^2 (>2 GeV)
- Angular resolution: < 0.2° (> 10 GeV)
- Energy resolution: ~2% (> 10 GeV)

Gamma-ray sky map LE-γ trigger (E >1 GeV)

Gamma-ray sky map HE trigger (E>10 GeV)

Nov. 2015 – Dec. 2022

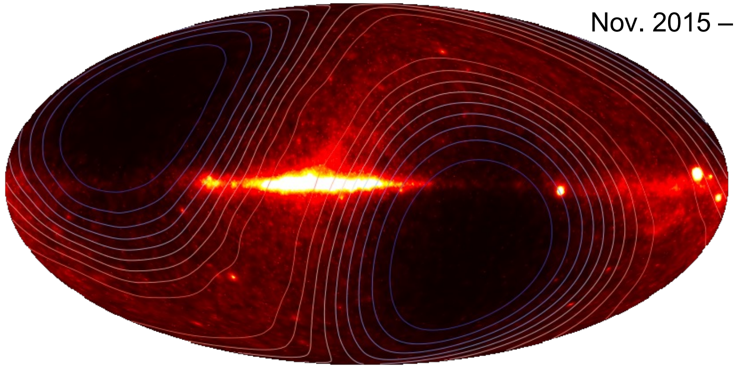

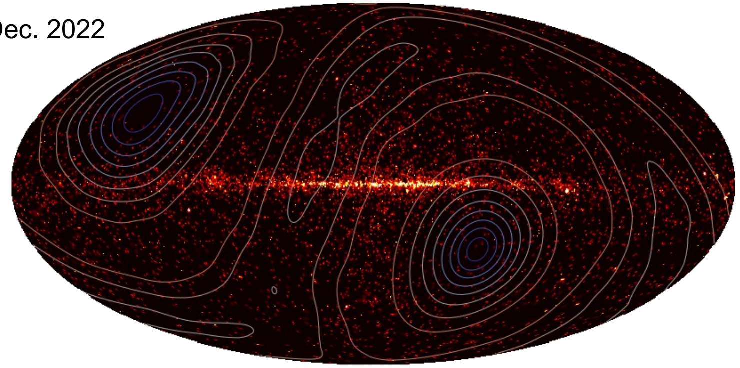

Energy spectra for bright point sources

Preliminary

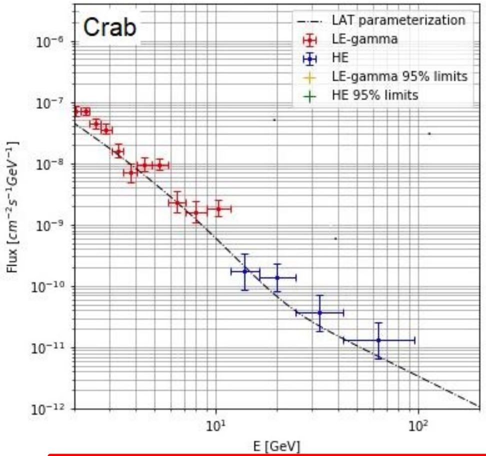

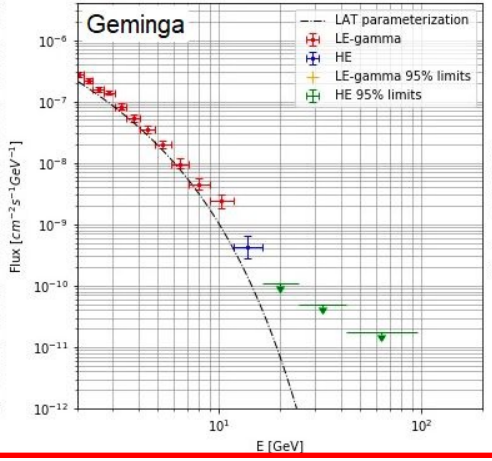

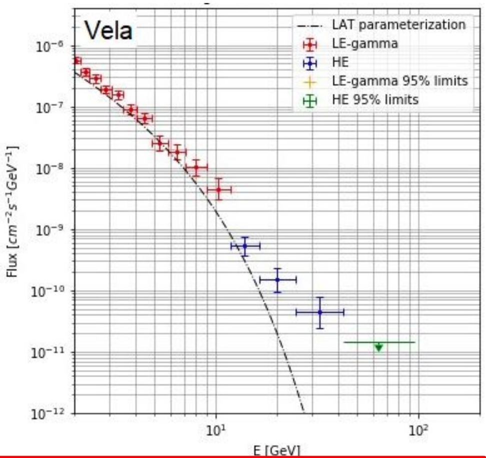

Gamma-ray spectrum

Preliminary

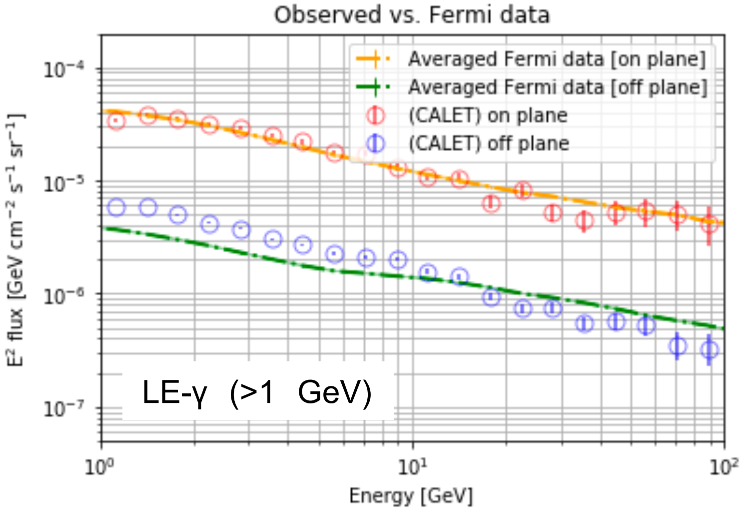

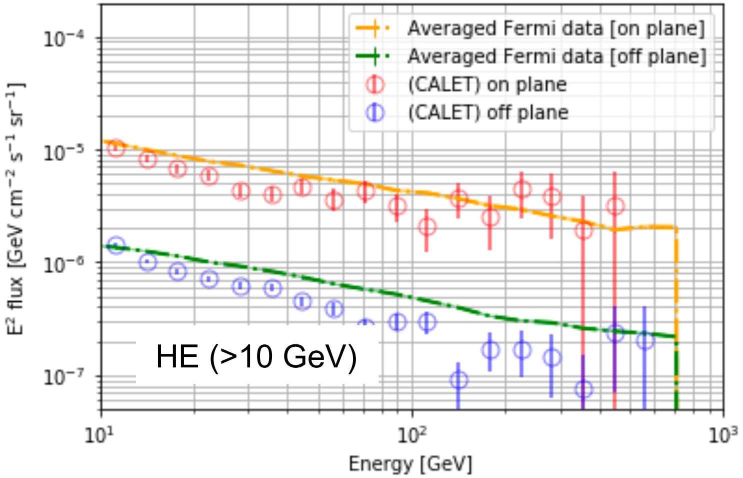

"**On-plane**": $|l| < 80°$ & $|b| < 8°$, "**Off-plane**": $|b| > 10°$

The spectra for point sources and diffuse components are found to be consistent with those by Fermi-LAT .

Gamma-ray Bursts and GW Follow-up

ApJ 933:85 (2022)

CGBM Specifications

	HXM	SGM
Crystal	LaBr3(Ce)	BGO
Number of detectors	2	1
Diameter [mm]	66.1 (small) 78.7 (large)	102
Thickness [mm]	12.7	76
Energy range [keV]	7-1000	40-20000
Field of view	~3 sr	~8 sr

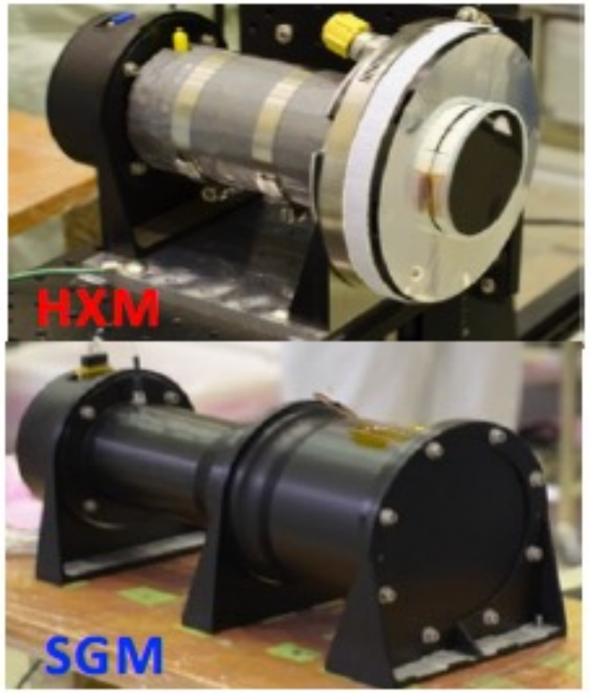

CGBM has detected 327 GRBs as of June 2023.

Duration distribution measured by SGM (40 – 1000 keV)

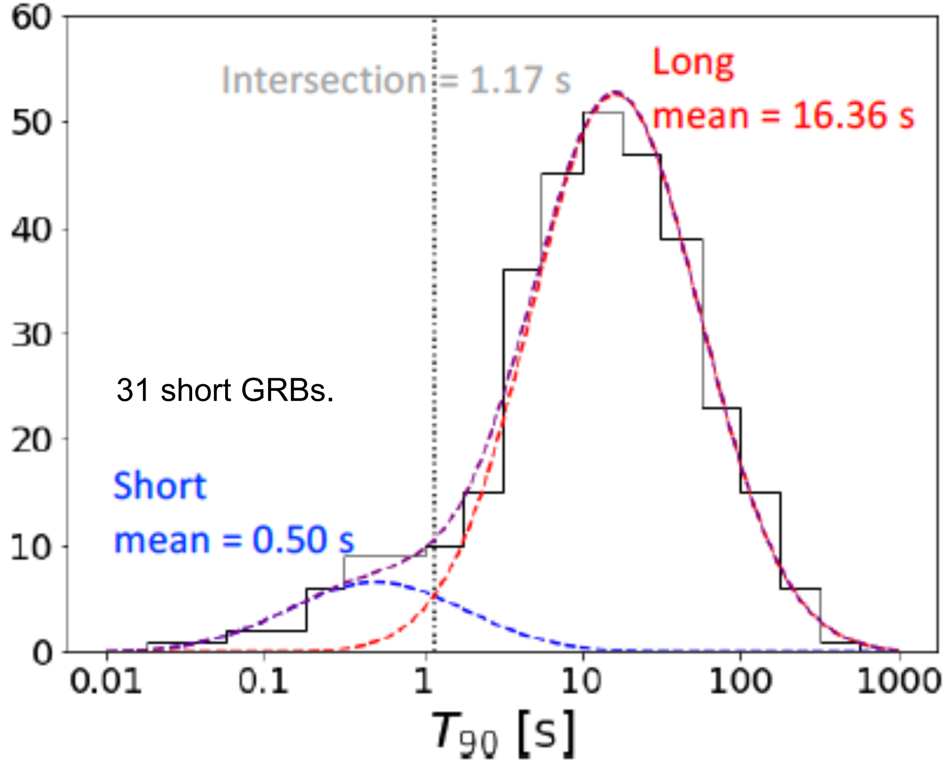

- **Follow-up** of LIGO/Virgo **GW** observations during O3 & O4
  - X-ray and gamma-ray bands
  - High-energy gamma-ray in the calorimeter

- We developed **automatic pipelines to process CGBM and CAL data** to analyze O4 events with higher event rates.
- **169 events have been reported via GCN Notice** in ER15 and O4, and the developed pipelines have been **triggered by LVC NOTICE and processed CALET data**, and enabled us to check many GW events.

Solar Modulation and Drift Model

PRL 130 211001 (2023)

Solar Modulation during Solar Cycles 24-25 Transition

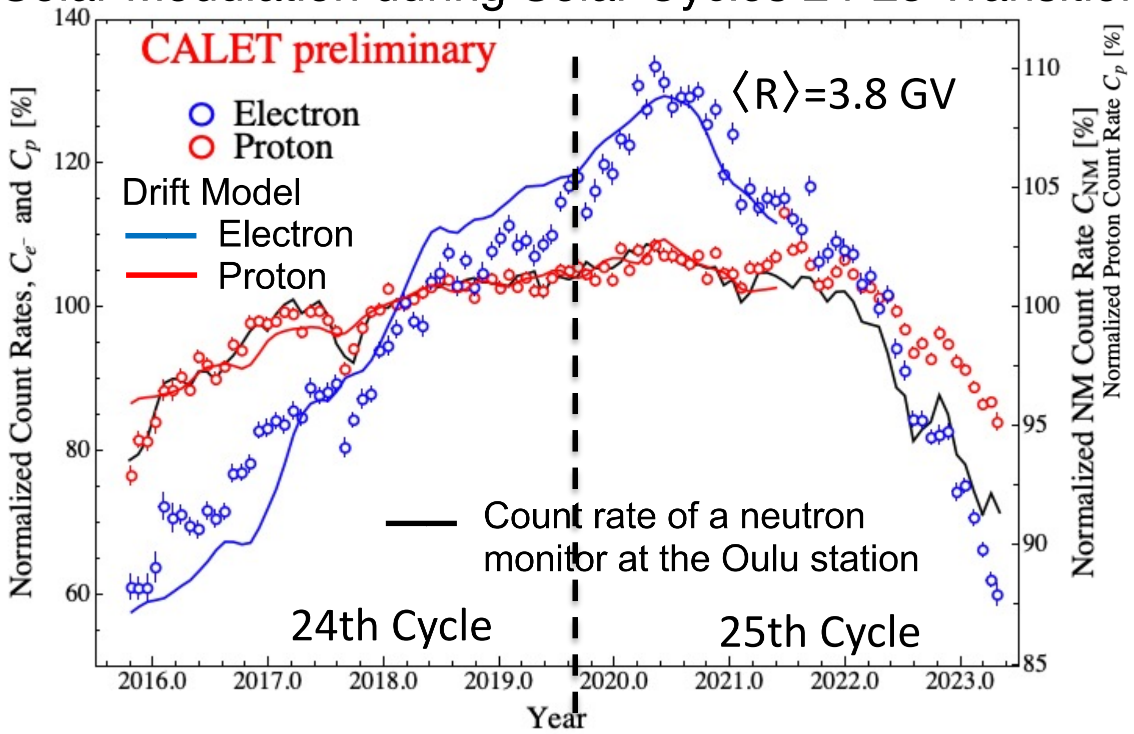

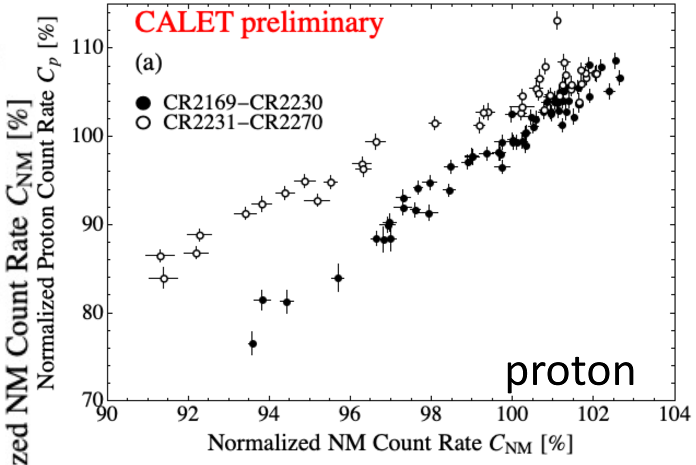

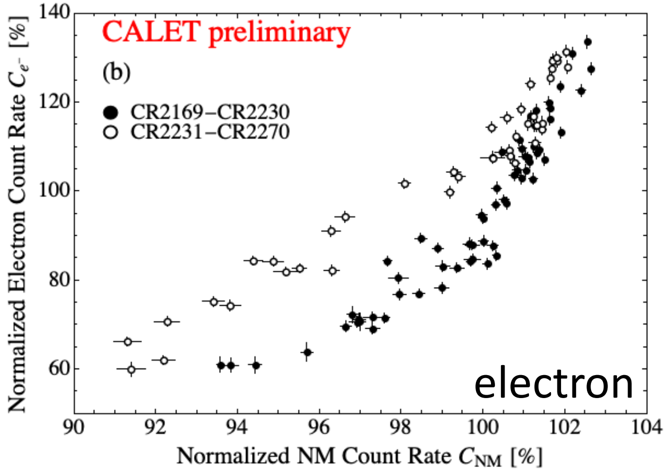

CALET proton (a) and electron (b) count rates at the average rigidity of 3.8 GV as a function of neutron monitor count rates at the Oulu station during the descending phase in the 24th solar cycle (closed circles) and the ascending phase in the 25th solar cycle (open circles).

- We have observed a clear charge-sign dependence of the solar modulation of GCRs, showing that variation amplitude of C_{e-} is much larger than that of C_p at the same average rigidity.
- We also have succeeded in reproducing variations of C_{e-} and C_p simultaneously with a numerical drift model of the solar modulation, which implies that the drift effect plays a major role in the long-term modulation of GCRs.
- We also find a clear difference between ratios, C_p/C_{NM}, during the descending phase of the 24th solar cycle and the ascending phase of the 25th solar cycle.

Summary and Future Prospects

- CALET was successfully launched on Aug. 19th, 2015. The observation campaign started on Oct. 13th, 2015. Excellent performance and remarkable stability of the instrument were confirmed in observations over 8 years.
- CALET is able to obtain precise measurements of the fluxes of CR electrons up to the TeV region, the energy spectra of CR nuclei from proton to nickel up to hundreds of TeV and secondary-to-primary ratios of individual elements, and contribute to multi-messenger astronomy by providing a precise knowledge of Galactic cosmic-rays.
- As a part of multi-messenger astronomy, CALET is carring out the observations of high-energy gamma-rays and gamma-ray bursts including GW follow-up, and is monitoring solar activities.
- Extended CALET operations were approved by JAXA/NASA/ASI in March 2021 through the end of 2024, and a further extension to 2030 is expected.

- ✓ *We greatly appreciate the JAXA staffs for perfect support of the CALET operations at the TKSC of JAXA !!*
- ✓ This work is partially supported by JSPS KAKENHI Kiban (S) Grant Number 19H05608 (2019-2023FY).

Thank you for your attention

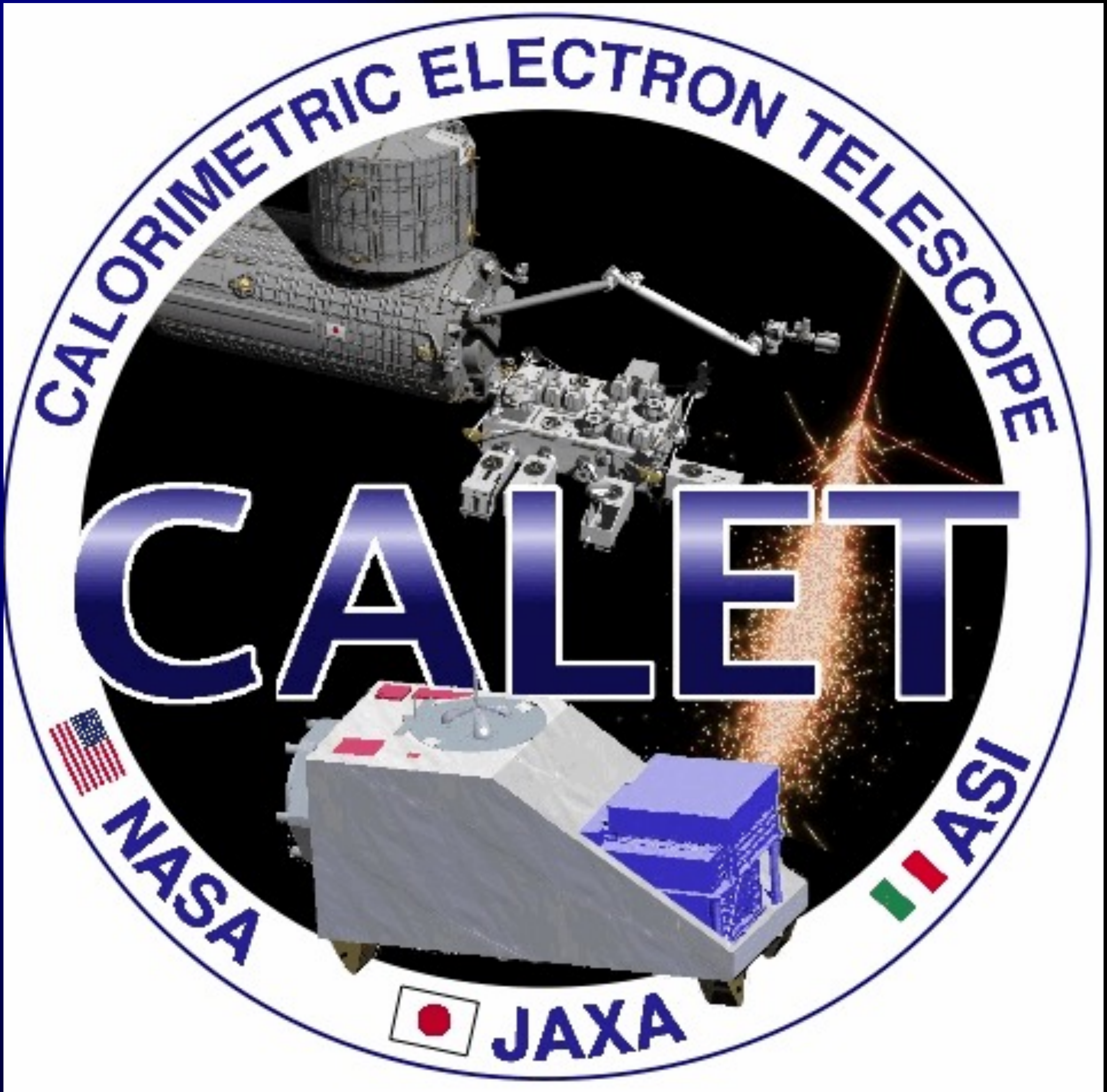

Publication List

- Operational over 2800 days with 86% live time, total triggers approaching 4 billion

Continuous on-orbit updates from ground calibration	Astropart. Phys. 91, 1 – 10 (2017)
Stable operations over a range of observing modes continue	Astropart. Phys. 100, 29 – 37 (2018)

- Analysis of CR events continues, extending to higher energies and charges

All-electron spectrum in the range 10 GeV – 7.5 TeV	PRL (2023) in press	(3rd update)
Proton spectrum in the range 50 GeV – 60 TeV	PRL 129, 101102 (2022)	(2^{nd} update)
Carbon and oxygen spectra in the range 10 GeV/n – 2.2 TeV/n	PRL 125, 251102 (2020)	1^{st} paper
Iron spectrum in the range 50 GeV/n – 2 TeV/n	PRL 126, 241101 (2021)	1^{st} paper
Nickel spectrum in the range 8.8 GeV/n – 240 GeV/n	PRL 128, 131103 (2022)	1^{st} paper
Boron spectrum in the range 8.4 GeV/n – 3.8 TeV/n	PRL 129, 251103 (2022)	new
Helium spectrum in the range 40 GeV – 250 TeV	PRL 130, 171002 (2023)	new
Preliminary analysis of ultra-heavy cosmic-ray abundances	see W.Zober CRD3-06 (ICRC2023)	preliminary

- Analysis of gamma-ray sources and transients continues

Calorimeter instrument response characterized	ApJS 238:5 (2018)
GW follow-up and GRB analysis with CGBM & CAL	ApJL 829:L20 (2016)
Counterpart search in LIGO/Virgo O3 with CGBM & CAL	ApJ 933:85 (2022)

- Analysis of transient heliospheric and space weather phenomena underway

Charge-sign dependence of Solar modulation	PRL 130, 211001 (2023)	new
Solar energetic particle and relativistic electron precipitation events	see A.Ficklin PCRD2-14(ICRC2023)	